Report 14, 1993

APPLICATION OF Cl, B TRACERS AND GEOINDICATORS TO DELINEATE SOME PRODUCTION CHARACTERISTICS OF MT. LABO GEOTHERMAL SYSTEM, PHILIPPINES

Dennis R. Sanchez,
UNU Geothermal Training Programme,
Orkustofnun - National Energy Authority
Grensasvegur 9,
108 Reykjavik,
ICELAND

Permanent address:
Geothermal Division,
PNOC-Energy Development Corporation,
PNPC Complex, Merritt Road, Ft. Bonifacio,
Makati, Metro Manila,
PHILIPPINES

ABSTRACT

This report focuses on the interpretation of water chemistry in the Mt. Labo area with the aim of delineating the characteristics of the Mt. Labo geothermal system. The types of waters in the area are: a) dilute neutral pH warm springs, b) alkaline Cl hot springs, c) acid to neutral pH SO_4-Cl warm springs, d) slightly acid (pH 5.1 at 270°C) Cl well waters, with relatively high SO_4.

The source of Cl and B in the warm spring waters is the rock with which these waters react. The main source of Cl in the other types of water is considered to be the magma heat source to the geothermal system. However, in these latter water types most of the B is derived from the dissolving rock. The SO_4-Cl warm springs are considered to form by the mixing of magmatic gases with surface waters, whereas the alkaline Cl hot spring waters and well fluids are formed by the mixing of magmatic gases at depth.

The pH of the aquifer water feeding the wells is calculated to be 5.1 at the aquifer temperature, 270°C. However, at the surface, the discharged waters are strongly acid (pH 3-4). The reason for this is relatively high SO_4 in the waters. Dissociation of HSO_4^- upon cooling in the well, as the water boils, is responsible for the low pH at the weirbox. SO_2 from magmatic gas is thought to be responsible for the relatively high SO_4 in the well waters.

The acid to neutral pH SO_4-Cl waters are relatively far from equilibrium for secondary minerals. Therefore, geothermometry results for these waters are not considered to be reliable. Quartz equilibrium temperatures (266-270°C) of the well discharges accurately match the measured temperatures, 270°C, indicating that equilibrium is attained with respect to quartz in the reservoir. Calculations also show that the well waters are close to saturation with calcite and anhydrite.

Substantial re-equilibration has occurred in the upflow with respect to the Na/K geothermometer, as indicated by Na/K temperatures of about 260°C. These are lower than the measured temperature in the aquifer. The Cl-SiO_2 relationship in the wells and the Kilbay-Alawihaw hot springs indicates that the hot spring waters have lost a substantial fraction of their SiO_2 by precipitation in the upflow, suggesting that quartz equilibrium temperatures are low for these hot springs.

It is not known if the Kilbay-Alawihaw hot springs have the same heat source as the exploration wells or a separate one. If there is a common heat source, cooling has occurred during lateral flow from the heat source to the hot springs. If this is the case, drilling at Kilbay-Alawihaw hot springs site may not yield temperatures in excess of 130°C, which are indicated by the quartz geothermometer. If, on the other hand, the Kilbay-Alawihaw hot springs have their own heat source, deep drilling at this site is expected to yield temperatures in excess of the quartz geothermometry temperature.

TABLE OF CONTENTS

LIST OF FIGURES

LIST OF TABLES

1. INTRODUCTION

The use of geochemical methods has played a crucial part in many geothermal exploration projects (e.g. Arnorsson, 1991; D'Amore, 1991; Giggenbach, 1991; Fournier, 1991; Reed, 1991; Truesdell, 1991). During the surface exploration phase of geothermal development, geochemistry may provide information on conditions and processes at depth that is not obtainable by geological and geophysical techniques. After all, the waters and gases discharged at the surface "have been there" and generally carry imprints of their deeper histories with them. The constituents encountered in these fluids may be subdivided into two major groups according to the type of information provided (Giggenbach, 1991).

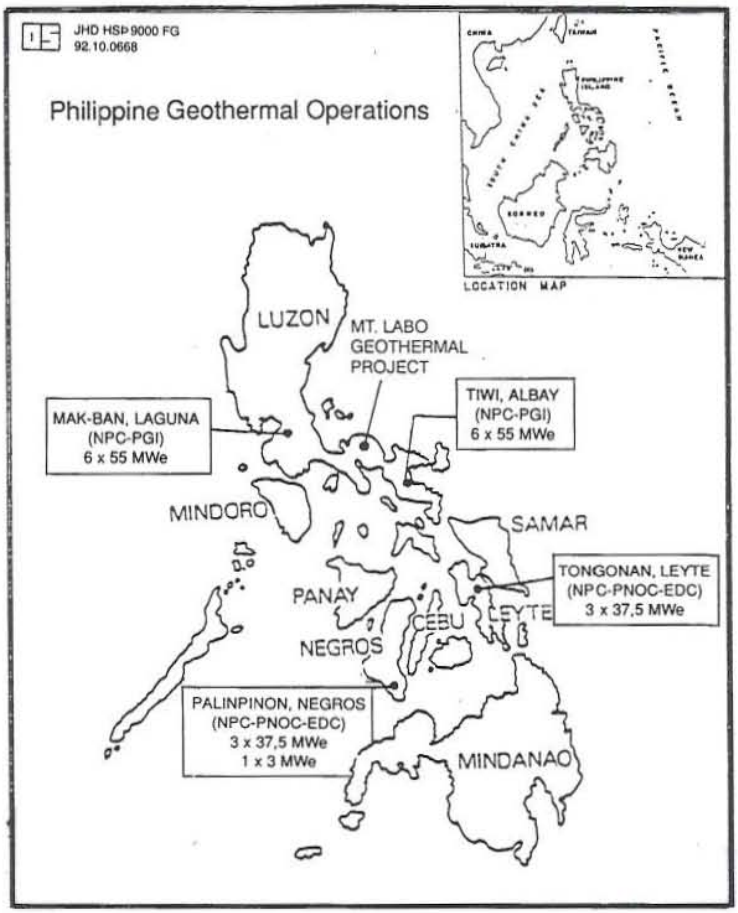

FIGURE 1: Location of Mt. Labo geothermal project and present geothermal production operations in the Philippines

Chemically inert, non-reactive and mobile constituents form a group called *tracers*. Once in the fluid phase, they should ideally remain unchanged, providing a tag and allowing their origins to be traced back to their source components. Examples of these are the noble gases He and Ar, followed by the comparatively "conservative" constituents Cl, B, Li, Rb, Cs, and N_2. Chemically reactive species, responding to changes in their environment in a controlled and well understood manner, form a group called *geoindicators*. Examples of these are Na, K, Mg, Ca, and SiO_2. They take part in temperature-dependent chemical interactions in the geothermal systems. In the present study, the behaviour of the Cl and B tracers, and of several geoindicators is assessed and subsequently applied to delineate the chemical characteristics of the recently drilled geothermal field at Mt. Labo in the Philippines. The field is located in the province of Camarines Norte at the Northern tip of the Bicol peninsula in southeastern Luzon (Figure 1). Locations of sampled springs and wells are shown in Figure 2. Previous geochemical studies that have been carried out in the area cover non-thermal waters including rivers and springs, thermal springs (Clemente, 1990), and geothermal well fluids (Gerardo, 1993; Sanchez, 1993). The following questions are specifically addressed in this study:

1) What can the chemistry of the fluids tell about their origin?
2) If the origin of the fluids could be differentiated, what sources are involved?
3) Which minerals control the activities of the geoindicators, and how closely are mineral/solution equilibria approached?

The water composition data selected to answer the above questions are from those presented by Clemente (1990), Gerardo (1993), and Sanchez (1993).

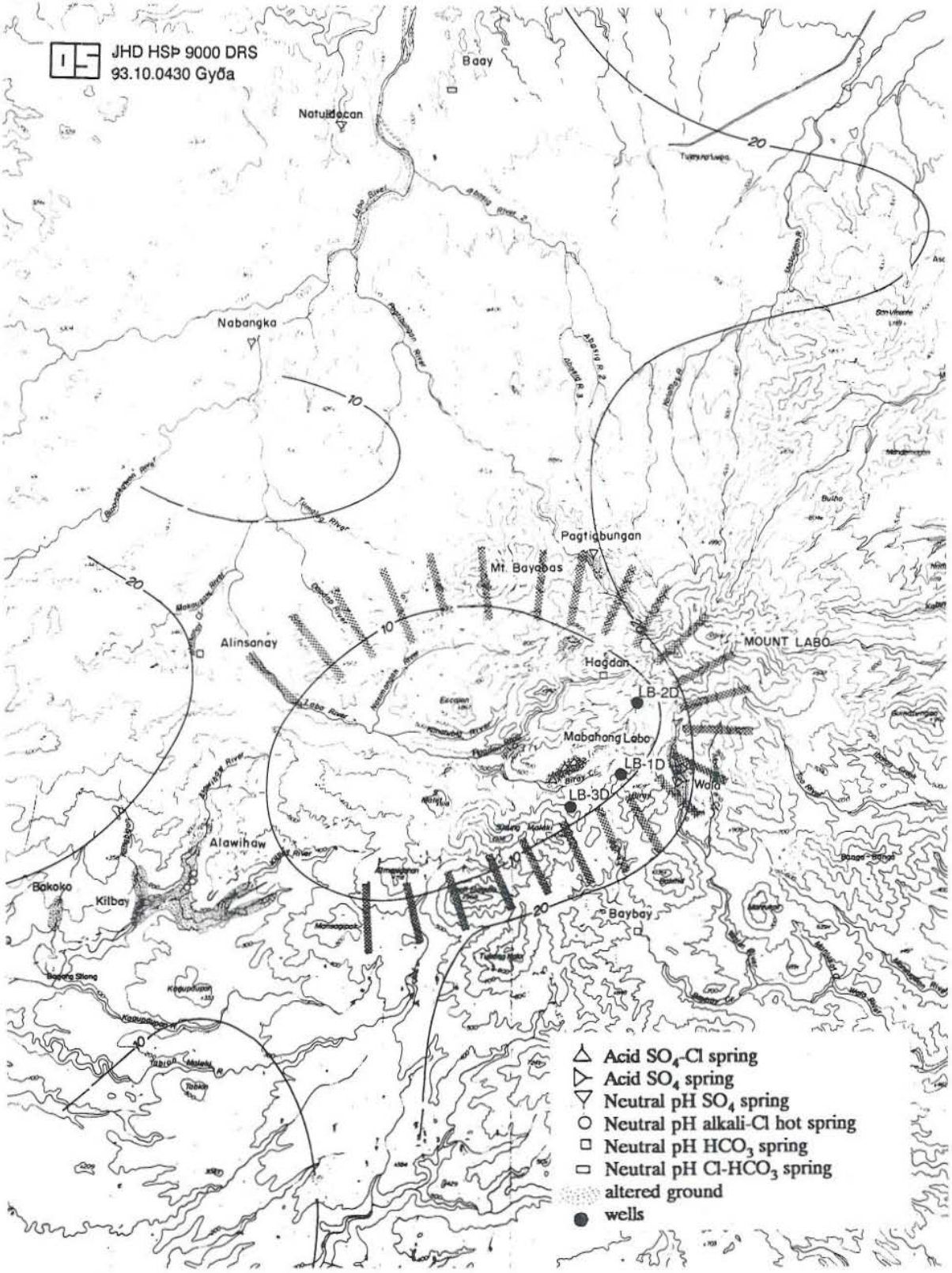

FIGURE 2: Location of sample points of natural waters in Mt. Labo, including rivers and springs, and of drilled wells in the area; encircled fence is the location of the upflow according to PNOC-EDC (1991). Also shown are resistivity contours in Ωm.

In all, 43 analyses from rivers and springs are used and 23 from wells, both downhole and discharge samples (Appendix I). The two exploration wells have only one dominant feed zone. Downhole measurements have been used to obtain the aquifer temperature.

2. GEOLOGY AND EXPLORATION DRILLING

2.1 Surface geology

Mt. Labo is the northernmost volcano in the Bicol Volcanic belt, a 200 km long chain of stratovolcanoes in southeastern Luzon (Figure 3). It is one of two inactive volcanoes (the other is Caayunan) comprising the Quaternary Labo volcanic complex (Delfin and Alincastre, 1988).

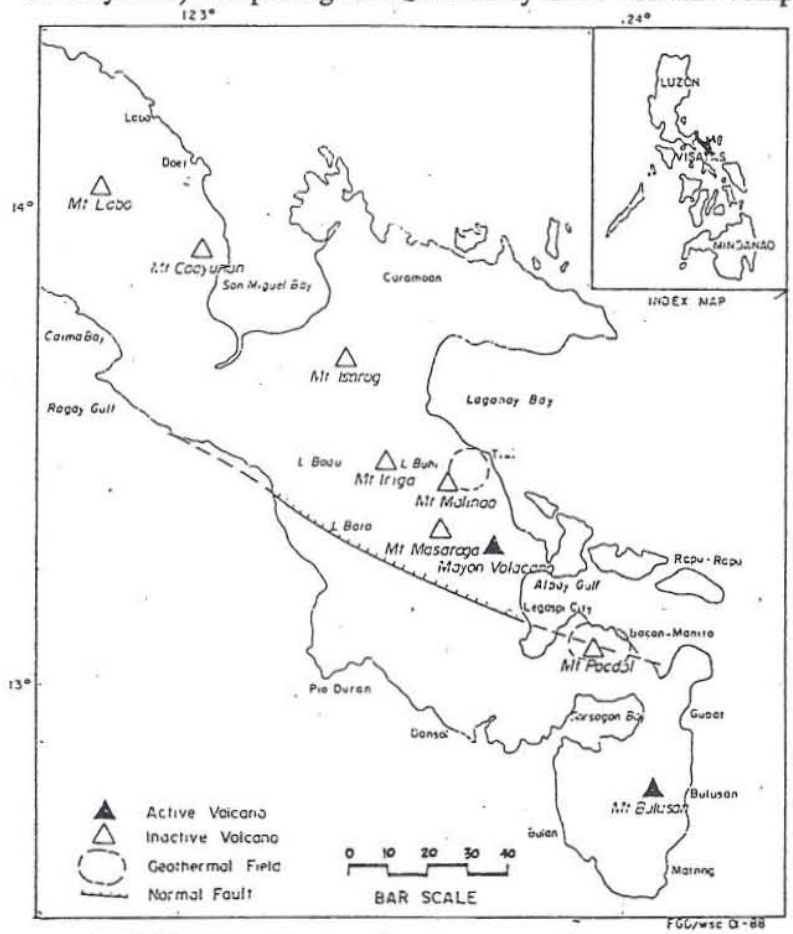

FIGURE 3: Series of quaternary volcanoes and geothermal fields in the southeastern Philippines (from Delfin and Alincastre, 1988)

The regional basement consists of Pre-Cretaceous and Cretaceous metamorphics and Cretaceous ultramafics found north and west of Mt. Labo. This basement is unconformably overlain by Tertiary rocks, which are intruded by Palaeocene granodiorite and Middle Miocene diorite intrusives. The geological map and the stratigraphic column of the Mt. Labo geothermal area are shown in Figures 4 and 5, respectively. The oldest rocks are the Upper Miocene Susung Dalaga Volcanic Formation found west of Mt. Labo. They consist of lava flows, agglomerates, and tuffs, mainly andesitic in composition.

Unconformably overlying these volcanics is a Pliocene sequence of shallow-marine sedimentary rocks belonging to the Vinas Formation (termed as clastic by Tebar and Apuada, 1985). Outcrops of this formation in the area consist of sandstones, poorly to highly fossiliferous air-fall tuff, calcisiltite, and metamorphosed limestones (PNOC-EDC, 1991).

The Labo volcanic formation, product of the Pleistocene Mt. Labo volcano, constitutes the youngest and most widespread rock unit in the area. The volcanic deposits, dating from 0.08-0.6 m.y. ago, are most likely associated with the present thermal activity at Mt. Labo (Delfin and Alincastre, 1988). This formation is subdivided into four informal members. The oldest and most extensive member is the basalt unit consisting of weathered and variably altered andesite, dacite, and basalt lavas and lahars. Erupted from the same magma source as the basalt unit are numerous lava domes of hornblende-andesite composition. These are distributed throughout the field with the largest number found southwest of Mt. Labo. The central cone of Mt. Labo overlies the basalt unit and possibly some lava domes. It is built largely of andesite and dacite lavas and laharic breccias. Pyroclastic flows on the northern flank of Mt. Labo make up the youngest unit. They consist of two non-bedded, poorly sorted, and poorly-consolidated to well-compacted andesite and dacite block and ash flows that erupted about 80,000 years ago (PNOC-EDC, 1991).

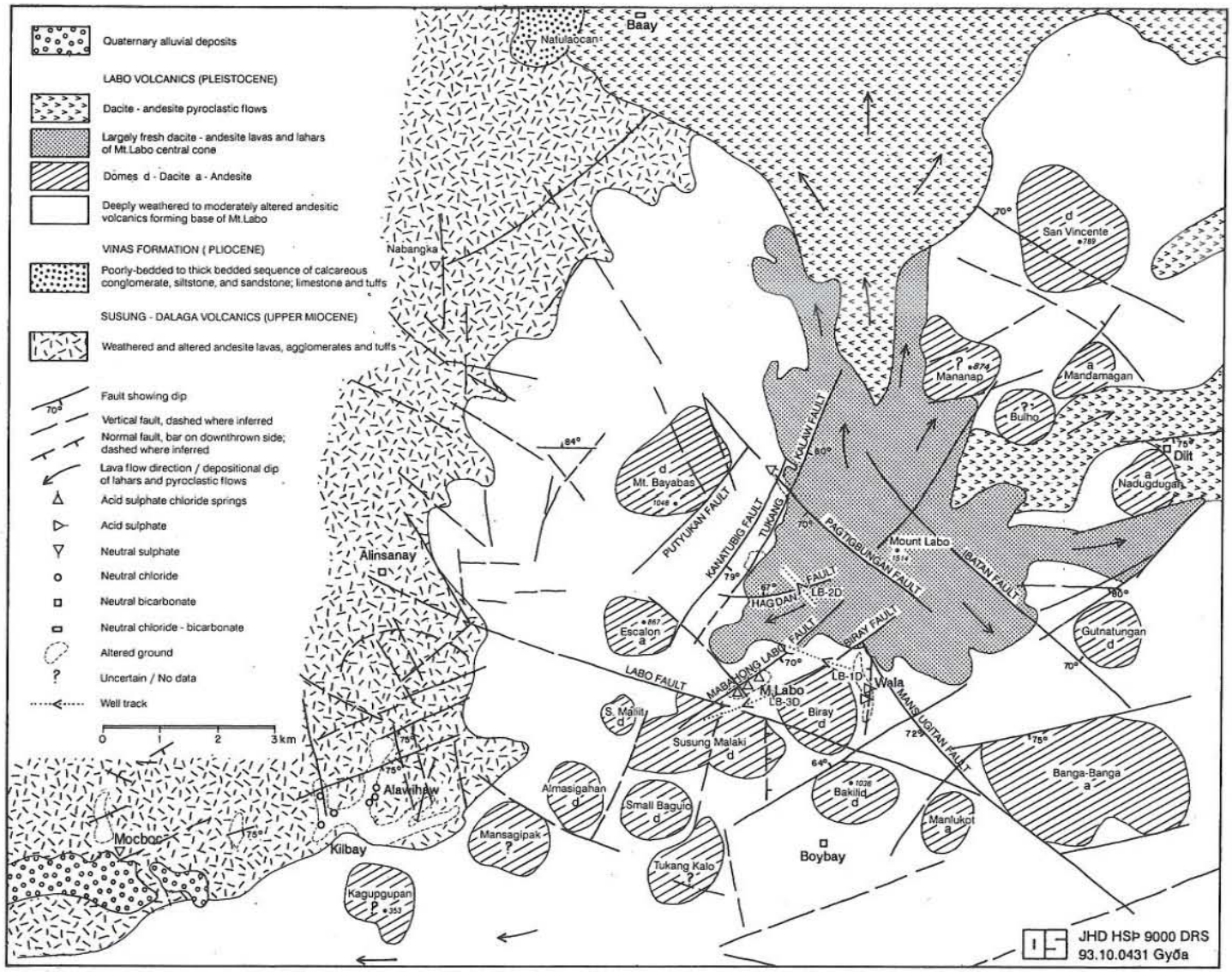

FIGURE 4: Geological map showing fault-structures, geothermal manifestations and types of rock in Mt. Labo (Delfin and Alincastre, 1988)

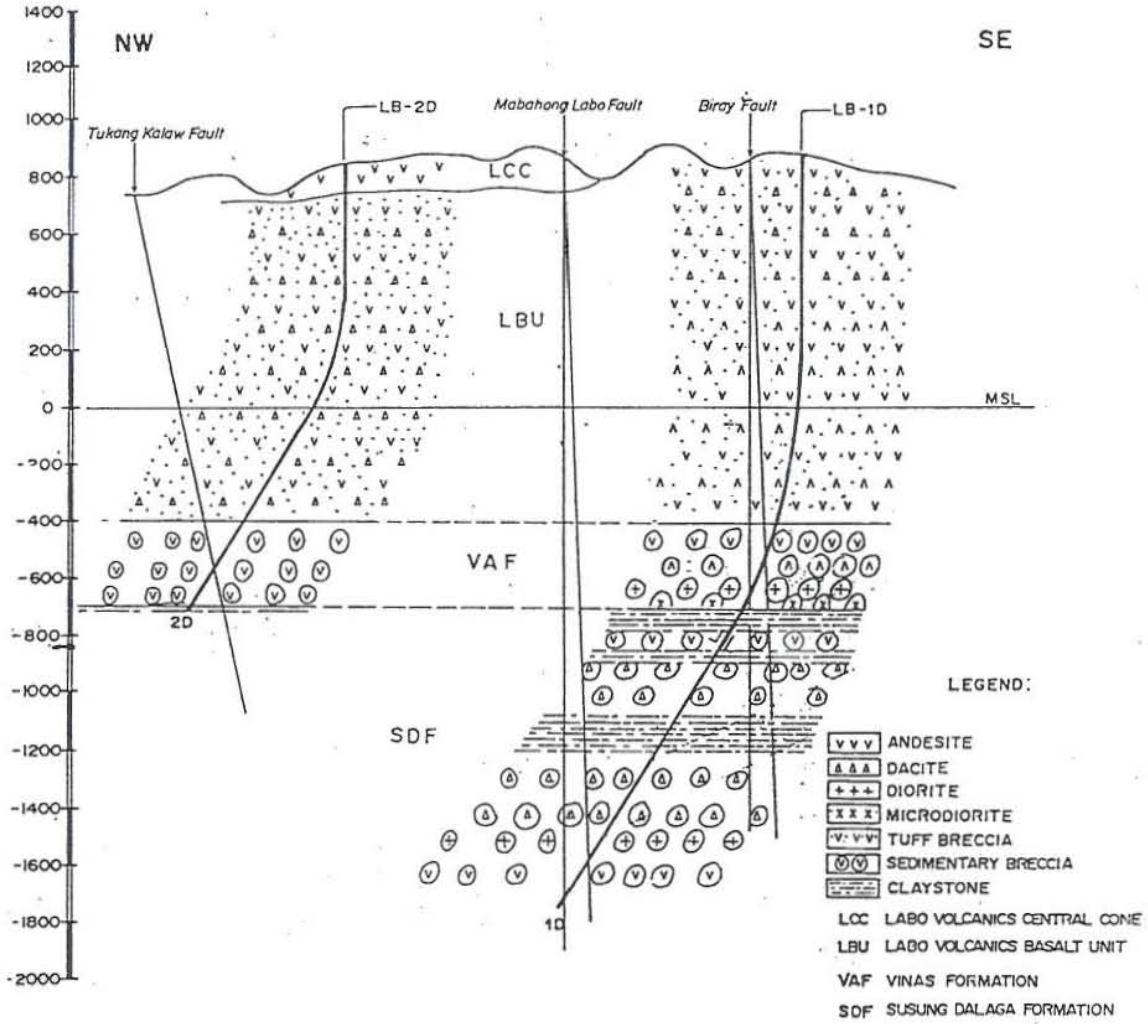

FIGURE 5: Geological stratigraphy of the Labo wells showing structures and lithological units (from PNOC-EDC, 1991)

Delfin and Alincastre (1988) consider the area to be cut by three major northwest and northeast trending dip-slip faults. The three major faults, the Ibatan, Pagtigbungan, and Labo Faults, define a pair of adjoining horst and graben-like blocks in the summit and southern flank of Mt. Labo. The eastern half of this 2.5-5 km wide graben is transected by several closely spaced northeast striking faults. The resulting configuration is a series of narrow, northeast-trending fault blocks within, and occasionally cutting through, the northwest-trending graben. Nearly half of all the thermal springs in the area are found within this graben or its projected extension. Most are localized along or near the traces of the northeast-striking faults, suggesting that these sets of structures control the flow of the rising geothermal fluids (Figure 4).

2.2 Exploration drilling and subsurface geology

Based on surface explorations (Delfin and Alincastre, 1988; Layugan et al., 1988), two exploratory wells were located in the inferred upflow region and drilled in the period May 1990 to January 1991. A third well, the drilling of which commenced in June, 1992, was also sunk in the inferred upflow (Figure 2). LB-1D was completed to a vertical depth (VD) of 2608 m (1738 m b.s.l.). LB-2D was prematurely terminated due to persistent drilling problems. It was plugged and

abandoned at a depth of 1618 mVD (758 m b.s.l.) with no production casing shoe. LB-3D was completed in September, 1992 at a total depth of 2413 mVD (1608 m b.s.l.) (Ramos et al., 1992). From the 1991 evaluation of the area (PNOC-EDC, 1991), the geological stratigraphy and lithology were revealed and are, in chronological order (see also Figure 5):

1. Susung Dalaga formation (Sdf)
2. Vina formation (Vaf)
3. Labo volcanic basalt unit (Lbu)
4. Labo volcanic central cone (Lcc)

The Susung Dalaga formation consists mainly of sedimentary breccia and fossiliferous carbonaceous claystone with minor sandstones and siltstone. Its clasts were intensely altered prior to erosion and incorporation in the formation. They include dacite, diorite, andesite, microdiorite, and rare serpentinite, which were probably derived from a landmass east of Camarines Norte during Late Miocene (BED, 1986). These clasts were deposited in a deep marine environment (Dizon, 1990). They are probably more than 1100 m thick.

The Vina formation is a unit of sedimentary breccia believed to be synchronous with the Pliocene Vinas formation mapped on the surface. Its clasts are also intensely altered andesites, diorite, microdiorite, quartz diorite, and dacite, all embedded in an argillaceous matrix. The absence of fossils and carbonaceous material in the 300 m thick formation differentiates it from the underlying formation.

The Labo volcanic basalt is the thickest unit, more than 1200 m, encountered by both LB-1D and LB-2D. It is composed of tuff breccia with crystal fragments of plagioclase, quartz, biotite, hornblende, pyroxene, cristobalite, tridymite, laumontite, illite, and magnetite; and altered lithic fragments of andesite, dacite, and tuff, all embedded in tuffaceous matrix. The unit, dated as Pleistocene or 0.58 Ma (Delfin and Alincastre, 1988), conformably overlies the Pliocene Vinas Formation.

The Labo volcanic central cone is made of fresh to slightly weathered biotite-bearing two-pyroxene oxyhornblende andesite lavas and pyroclastics and is about 200 m thick.

LB-1D was deviated to the northwest and intersected the Mabahong Labo Fault, the inferred permeable zone, at 2500 mVD (1600-1700 m b.s.l.), within the Susung Dalaga sedimentary breccia formation. The zone is characterized by recent acid alteration (alunite and diaspore). A second minor permeable zone, the Biray Fault is located at 900 mVD (600-700 m b.s.l.), within the Vina sedimentary formation (PNOC-EDC, 1991). This zone is characterized by neutral pH alteration minerals (Panem et al., 1990).

LB-3D lies 1.8 km west-southwest of LB-1D. Two permeable zones were encountered, at 2100 mVD (1400-1500 m b.s.l.) and at 2300 mVD (1450-1530 m b.s.l.). The latter zone is the Mabahong Labo Fault, considered the major feed zone. This is the same fault as that intersected by LB-1D. Both zones are in the Susung Dalaga sedimentary breccia formations. No acid alteration minerals were found in either feed zone (Ramos et al., 1993).

From the completion test data of LB-3D, it was inferred that a high permeability loss encountered at the well bottom at 2254 mVD (1502 m b.s.l.) is associated with the Mabahong Labo Fault.

3. SUMMARY OF PREVIOUS GEOCHEMICAL WORK IN THE AREA

3.1 Hot spring chemistry

The chemical composition of different water types in the Mt. Labo area is shown in Appendix I. The natural springs in the area include neutral pH Cl-HCO_3 warm springs, acid to neutral pH SO_4-Cl hot springs (35-50°C), and neutral pH alkali Cl hot springs (45-90°C).

The springs discharging at high elevation, namely Hagdan, Wala, Pagtigbungan, Mabahong Labo, Alinsanay, and Baybay include both neutral pH HCO_3 and acid SO_4-Cl waters. These waters were considered by Clemente (1990) to be the products of the reaction between near-surface waters and the gases released by boiling of the deep neutral pH chloride geothermal fluids. The relatively high concentration of Cl in the waters discharged by some of the Mabahong Labo springs was considered to be a contribution from the neutral pH Cl reservoir channelled by the Mabahong Labo Fault. The neutral pH HCO_3 springs at Hagdan, which were considered to represent steam heated waters, show that the steam condensing in this area is already depleted in sulphide, implying that Hagdan has a relatively less direct communication with the ascending fluid than Mabahong Labo. The neutral pH HCO_3 springs at Baybay and Alinsanay, and the Cl-HCO_3 spring at Baay, were also considered to have less direct pathways than the Mabahong Labo springs.

Neutral pH sulphate waters occur in the lowlands at Nabangka, Natulduocan, and Mocboc. Instead of having been produced by the oxidation of H_2S gas, these waters are thought to be products of oxidation of sulphides leached out from the mineralized zones in the area (Clemente, 1990).

The neutral pH Cl-HCO_3 springs of Kilbay and Alawihaw represent the outflow portion of the geothermal system. Apart from the high Cl contents of these springs, the sulphate concentrations are also considerable which could be due to oxidation of the H_2S gas and dissolution of sulphide minerals. The HCO_3 concentrations of these springs are also high (500-800 ppm), and travertine is being deposited by most of these springs.

The molecular ratios of the chemical components suggest the upflow to be situated near the Mabahong Labo area and the outflow to be at Kilbay-Alawihaw (Clemente, 1990). The molecular ratios also imply high source temperatures for the neutral pH Cl-HCO_3 springs of Alawihaw and Kilbay, in the range of 170-210°C (Clemente, 1990).

3.2 Fluid chemistry of exploration wells

Wells LB-1D and LB-3D were discharged in October and in November, 1992, respectively. LB-1D, which was completed in September, 1990, had failed to discharge after a series of stimulation operations (Gerardo, 1993). With an absence of substantial discharge chemistry data from LB-1D, two sets of downhole samples were collected to obtain preliminary geochemical data from the well. The first set was collected in November, 1990, and the second set in August, 1992, prior to discharge. The well was successfully discharged in October, 1992, but it produced acid fluids from the beginning.

Both the discharge and downhole chemistry indicated that LB-1D is fed by an acid zone at 2500 mVD (1700 m b.s.l.) (Gerardo, 1993). It was also considered that a possible cold inflow is present through the Mabahong Labo Fault. This is indicated by hematite and goethite at 2500 mVD

(1700 m b.s.l.) (Panem, 1990). It has further been suggested that the acid fluids in this fault are the result of oxidation of H_2S to H_2SO_4 (Gerardo, 1993).

From the discharge chemistry of LB-3D, Sanchez (1993) concluded that a neutral pH Cl reservoir exists west-southwest of Mt. Labo. The well discharged neutral pH Cl fluids for more than four weeks, before becoming acid (pH of weirbox samples less than 4.5). The acidity of the fluid from the well was considered to be due to the clearing of an acid feed zone, located at the well bottom and connected to the Mabahong Labo Fault. That this feed zone was potentially productive has been confirmed by recent borehole surveys. The sinker bar survey, conducted just after shutting the well, reached 2362 mVD (1575 m b.s.l.), about 70 m deeper than the previous maximum cleared depth of 2254 mVD (1503 m b.s.l.).

4. CHLORIDE AND BORON

4.1 Summary of the aqueous geochemistry of Cl and B in geothermal fluids

Truesdell (1975), Arnorsson et al., (1989), and Giggenbach (1991), have used the B and Cl contents of geothermal waters to obtain information on their origin. The B and Cl contents of hot springs have also been used to estimate the mixing of hot and cold waters in upflow zones of geothermal systems (Ellis, 1970; White, 1970; Fournier, 1977, 1979; Arnorsson, 1970, 1985; Stefansson and Arnorsson, 1975; Truesdell, 1991).

Experimental work on water-rock interaction at high temperatures revealed that B and Cl are "soluble" elements (Ellis and Mahon, 1964, 1967; Seyfried et al., 1984; Spivack et al., 1987). In the water-igneous rock interaction experiments carried out by Ellis and Mahon (1964, 1967), at 300 to 600°C, it was observed that a substantial fraction of B in the rock was dissolved within 1-2 weeks. However, at low temperatures (100 to 150°C) there is evidence that B is taken up from solution into the rock, into clay minerals, such as illite and mica (Harder, 1963; Palmer et al., 1987).

In natural rock-water systems Cl behaves essentially as a "soluble" element and, like B, is easily dissolved almost quantitatively in a few days from common igneous rocks at 300-600°C (Ellis and Mahon, 1964, 1967). It is considered that Cl does not enter the structure of the igneous minerals but occurs as soluble salts on their surfaces.

Cl and B concentrations in rain water, surface waters, and non-thermal groundwaters are considerably lower than in thermal waters. According to Arnorsson et al. (1993) B ranges from less than 0.01 ppm to a few ppm in these waters, but Cl from less than 1 ppm to several tens of ppm.

The Cl/B mass ratio in natural waters ranges from as little as 1 to that of sea water (4350), or even higher (Ellis and Sewell, 1963; Arnorsson et al., 1989, 1993). The lowest values are found in waters associated with some marine sedimentary rocks, e.g. Ngawha, New Zealand (Ellis and Sewell, 1963) and with geothermal systems having a degassing magma heat source (White, 1970, Arnorsson et al., 1989). Apparently, most waters with temperatures in excess of about 100°C have Cl/B ratios similar to those of the associated rocks (e.g. Ellis and Sewell, 1963; Arnorsson et al., 1989). Waters of lower temperatures sometimes have higher ratios. In the case of New Zealand geothermal waters this was considered to result from preferential dissolution of Cl from rock relative to B at these low temperatures (Ellis and Sewell, 1963).

The calculated Cl/B mass ratio of degassing andesitic and dacitic magma ranges from 6.04 to 4276 (Symonds et al., 1987; Le Guern and Bernard, 1982; Symonds et al., 1992; Giggenbach and Matsuo, 1991; Symonds, Mizutani, and Briggs, pers. comm; Le Guern, pers. comm.). This large variation is attributed to variable Cl (as HCl gas). Degassing Cl ranges from 3.9 to 2144 ppm while boron is fairly constant, ranging from 0.486 to 0.626 ppm (Symonds, 1992).

A number of studies have been conducted to determine the abundance of B and Cl in andesitic rocks as compiled by Harder (1969) and Fuge (1974). The abundance of these elements has also been determined in a number of magmatic gases from volcanoes as compiled by Symonds (1992). Tables 1 and 2 summarize data on the Cl and B content of andesitic rock and andesitic and dacitic magma gas. The average Cl/B mass ratio of andesitic rock is 10, according to Table 1, and the average Cl concentration 200 ppm.

TABLE 1: Abundance of Cl and B in andesitic rock
according to the compilation by Harder (1969) and Fuge (1974)

Locality	No. of samples	Range	Average
Boron			
Greece			24
Siberia	86	7-88	20
Siberia	49	7-132	40
New Zealand	1		22
(This report)			20
Chloride			
Japan/USA	11	20-370	180
Germany	2	110; 200	155
USA	1	80-430	140
Japan	9	70-620	202
Japan	13	30-370	285
Compilation	17		166
(This report)			200

TABLE 2: Abundance of Cl and B in andesitic and dacitic magma gases
as compiled by Symonds (1992) from various authors

Locality/Volcano	Magma	Temp. (°C)	Cl (%mole)	B (%mole)	Cl/B mass ratio	References
USA/Augustine	andesite	870	5.87	0.0045	4276	(A)
Indonesia/Merapi	andesite	928	0.5723	0.0028	671	(B) & (C)
Japan/Showashinzan	dacite	800	0.0456	0.0056	26.74	(D) & (E)
Japan/Usu	dacite	649	0.01067	0.0058	6.04	(F) & (G)

References: A) Symonds et al. (1992); B) Symonds et al. (1987);
C) Le Guern and Bernard (1982); D) Nemeto et al. (1957);
E) Symonds, Mizutani, and Briggs (pers. comm);
F) Giggenbach and Matsuo (1991); G) Le Guern (pers. comm)

4.2 Application and interpretation

Arnorsson et al. (1993) have recently proposed a model to explain the origin and chemistry of Cl and B in the cold and thermal waters of the southern Lowlands of Iceland. In their model, they assumed seawater and rock to constitute the only sources of these elements. Furthermore, Cl and B were assumed to be dissolved from the rock in stoichiometric proportions. They used the model to estimate the relative contributions of the marine component and rock dissolution to the total Cl and B in the natural waters.

A similar method will be applied to Mt. Labo geothermal system, with the modification that magma degassing will replace seawater as one source of Cl and B. Mt. Labo is located far inland and the possibility of an active channel for seawater mixing is extremely remote. Any marine Cl

or B would thus have to be supplied by seawater spray or aerosol through precipitation.

The contribution of Cl and B to natural waters at Mt. Labo from degassing magma and rock dissolution can be calculated from the Cl/B ratios of these sources and the measured Cl and B concentrations in water samples. We have

$$Cl_w = Cl_r + Cl_m \tag{1}$$

$$B_w = B_r + B_m \tag{2}$$

$$\frac{Cl_r}{10} + \frac{Cl_m}{4276} = B_w \tag{3}$$

where Cl_w and B_w are the Cl and B of the waters as analyzed. Cl_r and B_r represent the part dissolved from the rock and Cl_m and B_m that coming from the degassing magma. Any contribution from the atmosphere is neglected.

Multiplying Equation 3 by 10 yields:

$$Cl_r + \frac{10Cl_m}{4276} = 10B_w \tag{4}$$

Subtracting Equation 4 from Equation 1 gives:

$$Cl_m(1 - \frac{10}{4276}) = Cl_w - 10B_w \tag{5}$$

thus

$$Cl_m \frac{4266}{4276} = Cl_w - 10B_w$$

$$Cl_m = (Cl_w - 10B_w)\frac{4276}{4266} \tag{6}$$

Equation 6 could be expressed more generally as:

$$Cl_m = (Cl_w - RB_w)\frac{M}{M-R} \quad where \quad M>R \tag{7}$$

$$Cl_m = (Cl_w - RB_w)P \quad where \quad P = \frac{M}{M-R} \quad and \quad P>O \tag{8}$$

where R and M are the Cl/B mass ratios of the dissolving rock and the magma gases, respectively.

The closer the selected value of M is to that of R, the greater the magmatic contribution to the hydrothermal system for a given aqueous Cl/B ratio. This becomes evident by using the Cl_m/B_m

ratio of 671 (Le Guern and Bernard, 1982; Symonds et al., 1987) instead of the larger value of 4276 (Symonds et al., 1992), though both values are derived from data on gases from andesitic magma. If R is fixed at a value of 10, P becomes equal to 1.015 and 1.0023, respectively. It is apparent that the difference between the P values from the two andesitic Cl_m/B_m mass ratios is small (about 1.23%), and that the variation in the calculated Cl_m is governed by the Cl and B concentrations of the geothermal waters and not by the selected Cl/B ratio of the magma source. Therefore, Equation 8 gives similar results for different andesitic magma heat sources. In this report we used the M value of 4276 to estimate the minimum contribution of the degassing andesitic magma in the geothermal waters.

Figures 6 and 7 show the relation between Cl and B in samples from rivers/springs and well fluids, where Cl/B and B are plotted against Cl, respectively. The andesitic rock dissolution is delineated at a Cl/B ratio of 10. Similarly, the mixing lines from the degassing magma are also delineated. Two types of mixing were considered:

1. Mixing of magmatic gases with surface waters.
2. Mixing of magmatic gases with deep waters.

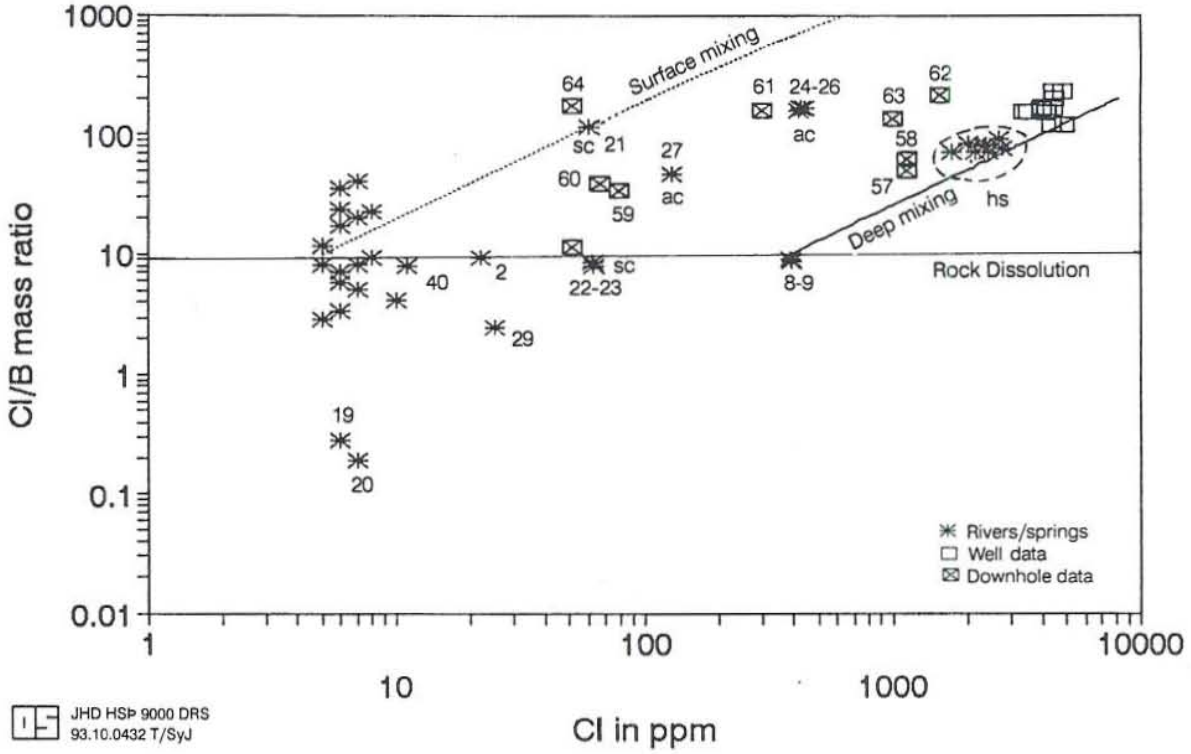

FIGURE 6: Distribution of Cl/B of Mt. Labo waters vs. Cl. The Cl and B in these waters is assumed to have originated from rock dissolution and degassing of the magma heat source. Rock dissolution is delineated at Cl/B equal to 10. The effect of the magmatic gas contribution on the Cl/B-Cl relationship in surface and deep waters is also shown. A Cl/B ratio of 4276 was assumed for the magmatic gases. The magmatic gases may mix with surface water or deep waters. (Spring waters that have significantly reacted with the rock and the degassing magma are labelled by a number code (see Appendix I) and **ac** (for acid pH SO_4-Cl spring), **sc** (for neutral pH SO_4-Cl spring), or **hs** (for neutral pH alkali-Cl hot spring); downhole samples are also labelled by a number code.)

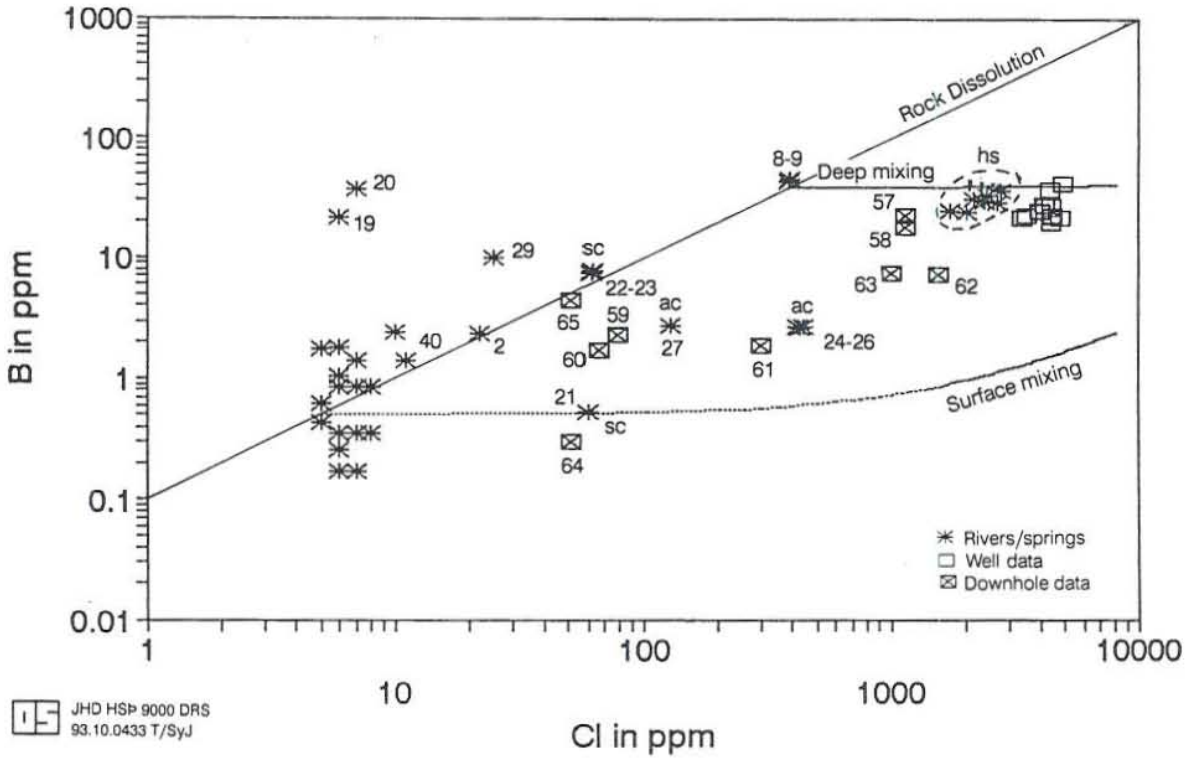

FIGURE 7: Distribution of B in Mt. Labo waters vs. Cl; the same assumptions are made as in Figure 6. The B originating from the dissolving rock and degassing magma is evaluated from the Cl/B ratios of 10 and 4276, respectively. (The symbols and the codes are the same as in Figure 6)

4.2.1 Rock dissolution

The surface waters possess Cl/B ratios in the range of 0.2 to 40 with Cl less than 10 ppm. Their B content ranges from 0.1 to 2.0 ppm. The Cl values are typical for surface and non-thermal waters in many parts of the world, the Cl being largely derived from seawater spray and aerosols. However, the very low Cl/B ratios of these waters, compared to seawater (4350), indicate that they have reacted substantially with the rock, and that most of the B must come from the rock as must some of the Cl. The surface waters at Mt. Labo are represented by samples from Natulducan (3), Nabangka (4), Kagupgupan (10), Katigbigan (16), Kamposta (17), Manikpik seepage (18), Baybay (28), Wala (30-32), Hagdan (33-34), and all the river waters (34-38, 40, 42-43). They are represented by unlabelled asterisks in Figures 6 and 7. The fairly high B content of Alinsanay springs (19- 20) may be due to some decomposition of organic matter picked up by the waters, and may not be associated with any rock dissolution or thermal activity in the area.

The warm spring waters that are dominated by the rock dissolution process possess a Cl/B ratio of about 10, i.e. similar to andesitic rock. They include the springs in Mocboc (2), L. Mabahong Labo (22, 23), and Baay (8, 9). These waters have Cl concentrations ranging from 20 to 400 ppm, depending upon the degree of rock dissolution.

4.2.2 Mixing with magmatic gases

Magmatic gases mixing with surface waters

There are five springs that could be considered products of magmatic gases being mixed with surface waters. They are the U. Mabahong Labo springs, coded as 21 and 24-27; all are sulphate Cl springs. Spring 21 has a neutral pH while the rest have a pH of 3.1 to 3.5. Clemente (1990) considered their sulphates a product of near surface oxidation of H_2S (i.e. by atmospheric O_2), and the high Cl a contribution from the neutral pH Cl reservoir, channelled by the Mabahong Labo fault. In view of recent well data, however, this seems an unlikely source for the Cl, because the springs are located at a high elevation (550 to 650 m a.s.l.), the groundwater level is at least 100 m below the springs (Biniza, 1990), and the geothermal waters at depth have low pH (5.1).

In this study, the Mabahong Labo Fault is assumed to be "steam-filled" and to contain some magmatic gases. The influx of the surrounding groundwater is prevented by the passage of the steam through the fault. Thus, the magmatic gases can only mix with surface waters. The acid pH of some of these springs is due to the dissolution of SO_2 and HCl in surface waters. The neutral pH of sample No. 21 is explained by relatively extensive reaction with surface rock subsequent to the mixing process.

The surface mixing curves indicated in Figures 6 and 7 correspond to the addition of Cl and B from the magma source to surface waters containing 5 ppm of Cl with a Cl/B ratio of 10. The line is generated using

$$Cl/B = Cl_w/B_w = \frac{Cl_m + Cl_r}{B_r + \frac{Cl_m}{4276}} \qquad (9)$$

The Cl (5 ppm) and B (0.5 ppm) in surface waters are set as the initial values of Cl_r and B_r, respectively, to provide the baseline concentrations of these elements for surface mixing. Below is an example of calculations using Equation 9:

Cl_m	Cl_w	B_w	Cl/B
0	5	0.5	10
10	5 + 10	0.5 + 10/4276	29.86
20	5 + 20	0.5 + 20/4276	49.54

and so on.

The surface mixing curve in Figure 6 is obtained by plotting Cl/B vs. Cl_w, while in Figure 7, it is delineated by plotting B_w vs. Cl_w, using the values calculated above.

The waters of the acid to neutral pH SO_4-Cl springs at U. Mabahong Labo (21, 24-27) are considered to be products of the mixing of magmatic gases with surface waters. The Cl content of spring No. 21, in particular, is a direct result of the mixing of Cl from the magma with surface waters, but the neutral pH of this spring is caused by water-rock interaction subsequent to mixing. The dissolution of the magmatic gases SO_2 and HCl has turned the waters of springs 24-27 acid, causing considerable rock dissolution, which has raised the concentration of Cl. This explains why the data points for samples 24-27 fall below the surface mixing curve.

Magmatic gases mixing with deep waters

The well fluids (44-56) and the Kilbay-Alawihaw hot springs (5-7, and 11-15) could be considered products of the mixing of magmatic gases with deep waters. The low pH (5.1) of the well fluids is due to the dissolution of SO_2 and HCl gases that are channelled along the Mabahong Labo fault to the deep water. The mixing curve for the deep waters and the magmatic gases is generated from Equation 9. The initial values of Cl_r and B_r are set at 390 and 39 ppm, respectively. These are the Cl and B concentrations of Baay springs (8, 9). Below is a sample calculation of the mixing of magma gases and deep waters using Equation 9:

Cl_m	Cl_w	B_w	Cl/B
0	390	39	10
10	390 + 10	39 + 10/4276	10.26
20	390 + 20	39 + 20/4276	10.51

and so on.

The deep mixing curve in Figure 6 is delineated by plotting Cl_w/B_w against Cl_w, while in Figure 7, the mixing curve is delineated by plotting B_w against Cl_w.

The amount of Cl and B in the geothermal waters derived from magmatic gases

The degree of mixing of magmatic gases with surface and deep waters can be evaluated with the aid of Figures 6 and 7. In Figure 6, Cl/B is plotted against Cl, while B is plotted against Cl in Figure 7. Although Figure 6 could also be used to explain B in the fluids, the latter figure was presented to illustrate, in detail, the behaviour of B in these mixing processes.

The amount of Cl_m in the geothermal waters is computed by expressing Equation 9 in terms of Cl_m and Cl_w, where U is the calculated Cl_w/B_w mass ratio of the sample, and M (equal to 4276) and R (equal to 10) are the Cl/B mass ratios of andesitic magma gas and the andesitic rock, respectively:

$$Cl_m = Cl_w \frac{M(R-U)}{U(R-M)} \qquad (10)$$

B_m is computed by expressing Equation 9 in terms of B_m and B_w:

$$B_m = B_w \frac{U-R}{M-R} \qquad (11)$$

Subsequently, Cl_r and B_r are computed using Equations 1 and 2, respectively. A summary of the computed percentage of Cl and B in the Mt. Labo waters derived from rock dissolution and magmatic gases is presented in Table 3.

In Figure 6, spring No. 21 plots on the surface mixing curve. This indicates that the spring discharge is a mixture of magma gases and surface waters. The Cl content of this spring is largely derived from the degassing magma. The neutral pH of the water is considered to result from water-rock interaction subsequent to mixing of the magmatic gases. The amount of Cl originating from the magma, Cl_m, is 55 ppm, constituting 92% of the total Cl in the water. The acid SO_4-Cl springs are of similar origin. They are surface waters to which magmatic gases have been added. When SO_2 and HCl that accompany other magmatic gases dissolve in the water, it turns acid. In addition to the Cl that rock dissolution contributes, oxidation of the SO_2 produces H^+ and SO_4^{2-}.

TABLE 3: Summary of the calculated amount of Cl and B in natural waters at Mt. Labo deriving from a) the dissolving rock, and b) degassing magma

Source	No. Code	Cl_w	B_w	$U = Cl_w/B_w$	Cl_m	B_m	Cl_r	B_r	$\%Cl_m$	$\%B_r$
U. Mabahong Labo	21	60	0.52	115.4	55	0.013	5.1	0.51	92	98
U. Mabahong Labo	24	446	2.68	166.4	420	0.098	25.8	2.58	94	96
U. Mabahong Labo	25	427	2.59	164.9	402	0.094	25.0	2.50	94	96
U. Mabahong Labo	25	420	2.68	156.7	394	0.092	25.9	2.59	94	97
U. Mabahong Labo	27	128	2.73	46.9	101	0.024	27.1	2.71	79	99
Kilbay-Alawihaw hot springs (avg)	5 to 7 & 11 to 15	2312	29.55	78.2	2021	0.473	290.8	29.08	87	98
Wells (avg)	44 to 56	4240	26.00	163.1	3989	0.933	250.7	25.07	94	96
Downhole	57	1142	22.50	50.8	919	0.215	222.9	22.29	80	99
Downhole	58	1142	18.20	62.7	962	0.225	179.7	17.97	84	99
Downhole	59	79	2.30	34.3	56	0.013	22.9	2.29	71	99
Downhole	60	66	1.70	38.8	49	0.011	16.9	1.69	74	99
Downhole	61	299	1.90	157.4	281	0.066	18.3	1.83	94	97
Downhole	62	1547	7.30	211.9	1477	0.346	69.5	6.95	96	95
Downhole	63	1000	7.40	135.1	928	0.217	71.8	7.18	93	97
Downhole	64	52	0.30	173.3	49	0.011	2.9	0.29	94	96
Downhole	65	52	4.50	11.6	7	0.002	45.0	4.50	13	100

Note:
1. Cl_m and B_m are Cl and B from degassing magma.
2. Cl_r and B_r are Cl and B from rock dissolution.
3. Cl_w and B_w are Cl and B as analyzed.

The calculated value of Cl_m in acid springs 24-26 is about 400 ppm, corresponding to 94% of the total Cl in these waters. Spring 27 has lower Cl_m, about 100 ppm, corresponding to 78% of the total Cl and indicating that considerable rock dissolution has occurred, prior to or subsequent to mixing of the magmatic gases. It is apparent that the Cl content of these acid to neutral pH SO_4-Cl waters is primarily controlled by the supply from the magmatic source.

The source of supply of Cl and B in the fluids from the wells and Kilbay-Alawihaw hot springs could also be evaluated with the aid of Figure 6. The well fluids align near the deep degassing line. This indicates that much of the Cl (average: 4240 ppm) in the wells comes from mixing of magma gases and waters at depth. Here, the value of Cl_m is almost 4000 ppm, corresponding to about 94% of the total Cl.

Dilution of the geothermal water with drilling fluid, and possibly also shallow groundwaters, is considered to be responsible for the variable Cl of the downhole samples. Assuming the undiluted Cl_m value in the aquifer to be 1/100 ppm as suggested above, the values of Cl_w of downhole samples in LB-1D divided by 4000 are indicative of the dilution of the initial Cl_m. For example, Cl_m of sample 57 is 919 ppm, and its ratio over 4000 is about 0.23. The decrease of the Cl_m in sample 57, from the initial value of 4000 ppm, to 919 ppm, could only be explained by dilution. Thus, the percentage dilution of the downhole samples ranges from 63% to 99%.

The hot springs at Kilbay-Alawihaw have a different origin. Since they are surface manifestations, their very high Cl content (average of 2312 ppm) could either be due to extensive rock dissolution by acid SO_4-Cl waters, or to deep mixing of magmatic gases. If the former process is dominant, the acid waters would require a long residence time in the springs to dissolve the surface rocks. This seem unlikely. It is concluded that the high Cl of the springs and almost boiling temperatures could only be explained by deep mixing. The Cl_m in these springs is 2021 ppm, corresponding to about 87% of the total Cl. This indicates that the rock has supplied a considerable amount of Cl, either before mixing of magmatic gas with deep groundwater, or subsequent to it.

If the Cl_m of the Kilbay-Alawihaw hot springs is assumed to come from the same source as the Cl_m of the well fluids (Cl_m = 4000 ppm), the dilution of the Cl_m in the hot springs is about 50%. This assumes that the deep fluids around the wells flow laterally to the Kilbay-Alawihaw hot springs.

Figure 7 illustrates the behaviour of B. In spring No. 21, B concentrations are similar to those of surface waters. However, in springs 24-27, there is an additional supply of B from the rock as indicated by higher B concentrations and Cl/B ratios, which are intermediate to those of andesitic rock and andesitic magma gases. The B from the rock is about 2.5 ppm, constituting about 96 to 99% of the total B in the fluids. There is a very insignificant, if any, supply of this element from the degassing magma.

Figure 7 also illustrates the behaviour of B in the well fluids and in the hot springs, considered to have formed by the mixing of magmatic gases and water at depth. From this figure, it is seen that the B concentrations in these waters are relatively constant (B_w ranges from 26 to 30 ppm), and that most of it is derived from the rock (B_r ranges from 96 to 98%) with only a small portion from magmatic gases. The slightly higher B in the hot springs (B_w average of 30 ppm), as compared to 26 ppm of the well fluids, can be accounted for by steam loss and rock dissolution before or subsequent to mixing in the upflow. The B in the downhole samples is also primarily derived from the rock (96 to 100%).

From Figures 6 and 7, and from the calculated amounts of Cl and B derived from their assumed two sources, the rock and magma gases (Table 3), it is concluded that the Cl content of the acid to neutral pH SO_4-Cl springs of Mabahong Labo is largely controlled by magma degassing (79-94%). The Cl of the well fluids and Kilbay-Alawihaw hot springs is controlled by the same process (87-94%). B, however, is largely derived from the rock in all types of water (91-99%). Dilution by drilling fluids and shallow groundwater (ca. 63-99%), is responsible for the variable Cl and B content of the downhole samples.

5. GEOINDICATORS

5.1 Theory

Unlike tracers such as B and Cl, geoindicators take part in temperature dependent chemical interactions in the system. Their activities are controlled by certain minerals present in the rock, the solubilities of which are temperature dependent. Fournier (1991) classified the geoindicators that could be used as geothermometers into two groups: (1) those based on temperature dependent variations in solubility of individual minerals, and (2) those based on temperature-dependent exchange reactions that fix ratios of certain dissolved constituents. Within group 1, the silica minerals are ideal for geothermometry, while in group 2, common minerals are used, i.e. low-albite and K-feldspar minerals. In the latter case, two or more dissolved ionic species are required to calculate the temperature at which solution-mineral equilibrium was last attained.

The solubilities of all silica minerals decrease drastically below 340°C. Fournier (1973, 1991) observed that on a plot of the logarithm silica concentrations versus the reciprocal of the absolute temperature, the solubility data for quartz, chalcedony, alpha-cristobalite, opal-CT, and amorphous silica lie along nearly straight lines over the temperature range of 20 to 250°C. A number of studies on silica mineral solubility as a function of temperature (e.g. Fournier, 1977; Fournier and Potter, 1982) have been conducted and applied in predicting reservoir temperatures during the exploration phase in geothermal development.

Equilibrium constants for mineral-solution reactions involving more than one cation are expressed as specific cation ratios. The ratios, like the equilibrium constant, vary with temperature. A number of studies have been carried out on various cation ratios for geothermometry purposes such as Na/K (Fournier and Truesdell, 1973; Arnorsson et al., 1983; Giggenbach, 1988), K/Mg (Giggenbach, 1988), and Na/K/Ca (Fournier and Truesdell, 1973). These studies have proven to be a valuable tool, both in predicting subsurface temperatures and in investigating mineral-solution equilibria in geothermal systems.

5.2 Application and interpretation

Various studies indicate that rock dissolution, rather than mineral-solution equilibria, is the principal process affecting the composition of natural surface waters and cold groundwaters. As these waters seep into the ground and develop into geothermal fluids by gaining heat they attain saturation with respect to various hydrothermal minerals. Crossplots of specific geoindicators against a tracer for thermal and non-thermal water in a particular area can help assessing the state of evolution of the water, and in this way aid geothermometry interpretation. Such crossplots of SiO_2, Na, K, Mg, Ca, and carbonate vs. Cl are illustrated in Figures 8 to 13. A line of assumed "incompatible" behaviour, i.e. following stoichiometric dissolution, is delineated in every figure for each geoindicator, to illustrate the behaviour during the initial rock dissolution stage.

Table 4 presents the average abundances and the geoindicator ratios to Cl in andesitic rocks, based on McBirney (1984) and Hoefs (1974). The dissolution line for each geoindicator was generated by plotting the geoindicator/Cl ratio from an initial value of 5 ppm Cl (estimated concentration in local precipitation).

TABLE 4: Abundances of elements used as geoindicators (in ppm) and their respective ratios to the Cl of andesitic rock (data from McBirney, 1984, and Hoefs, 1975)

CO_2	-	800	CO_2/Cl	-	4
SiO_2	-	60400	SiO_2/Cl	-	3020
Ca	-	44300	Ca/Cl	-	222
Na	-	31900	Na/Cl	-	160
Mg	-	16885	Mg/Cl	-	84
Fe	-	49750	Fe/Cl	-	249
K	-	9960	K/Cl	-	50

To illustrate this, consider an increase in SiO_2 with the increase in Cl. From Table 4, it is seen that the SiO_2/Cl ratio is equal to 3020, hence:

Cl	SiO_2
5 + 10/3020	10
5 + 100/3020	100
5 + 1000/3020	1000

and so on.

5.2.1 Dissolution diagrams

From Figures 8 to 13, it can be seen that all the warm spring waters that have reacted significantly with the rock and the magmatic gases, as deduced from their Cl and B content (springs 2, 8, 9, 21, 22-27, 29, 40), as well as the hot spring and well fluids, are shifted away from the dissolution line. On the other hand, surface waters (unlabelled asterisk) align approximately along the dissolution lines, indicating that the activities of the geoindicators in surface waters are not controlled by mineral-solution equilibria, but by their dissolution from the rock.

The lateral shift of the warm and hot springs (labelled asterisk) and the well fluids away from the dissolution line could be due to: a) precipitation of the respective geoindicator species from solution to form secondary minerals, or, b) the addition of Cl to the water from the magma source, or, any combination of the two processes. The dissolution diagrams cannot differentiate or identify which process or processes are involved. However, certain salient features could be deduced using these diagrams.

In Figure 8, the data points for the neutral pH alkali-Cl hot springs (the hs group) do not align along the dilution line of the well fluids and downhole samples. This indicates that the SiO_2 of the hot springs could either be controlled by a different SiO_2 mineral, or, which seems more likely, the hot spring waters have lost silica in the upflow through precipitation. Therefore, quartz equilibrium temperatures for the hot springs will be low in relation to the actual aquifer temperatures.

In Figures 9 and 10, it is seen that Na and K of the neutral pH, alkali-Cl hot springs align along the dilution line of the wells, indicating that the Na and K concentrations of the hot spring waters are controlled by the same Na and K mineral equilibria as the well waters.

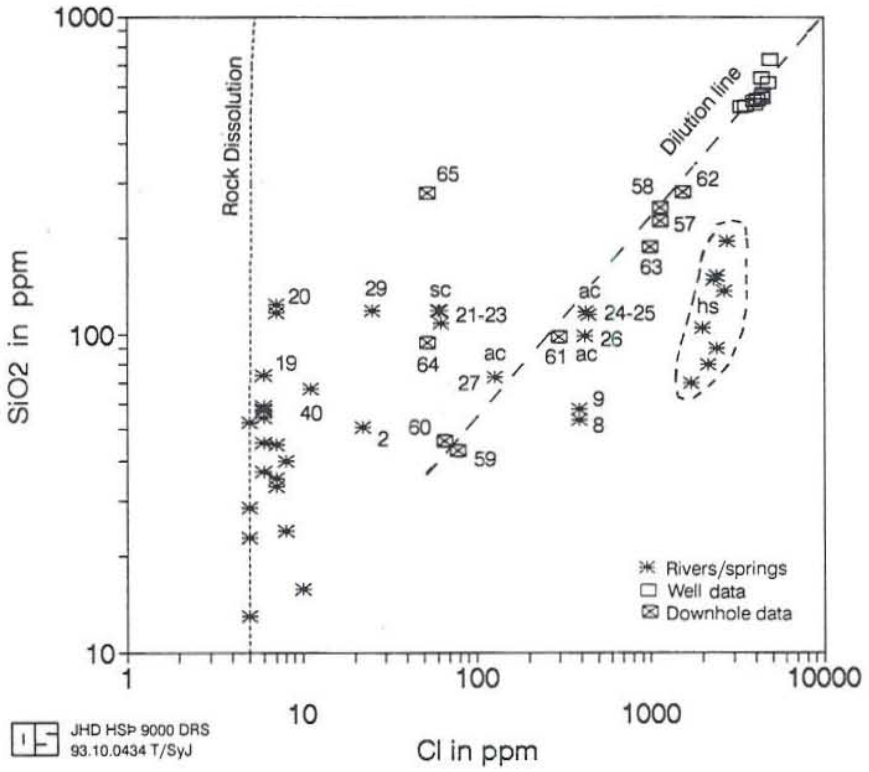

FIGURE 8: The distribution of SiO_2 vs. total Cl in natural waters at Mt. Labo; the slope of the line (3020) represents the ratio of SiO_2/Cl in andesitic rock. It is drawn through a value of 5 ppm Cl at zero SiO_2, the estimated Cl concentration in local precipitation

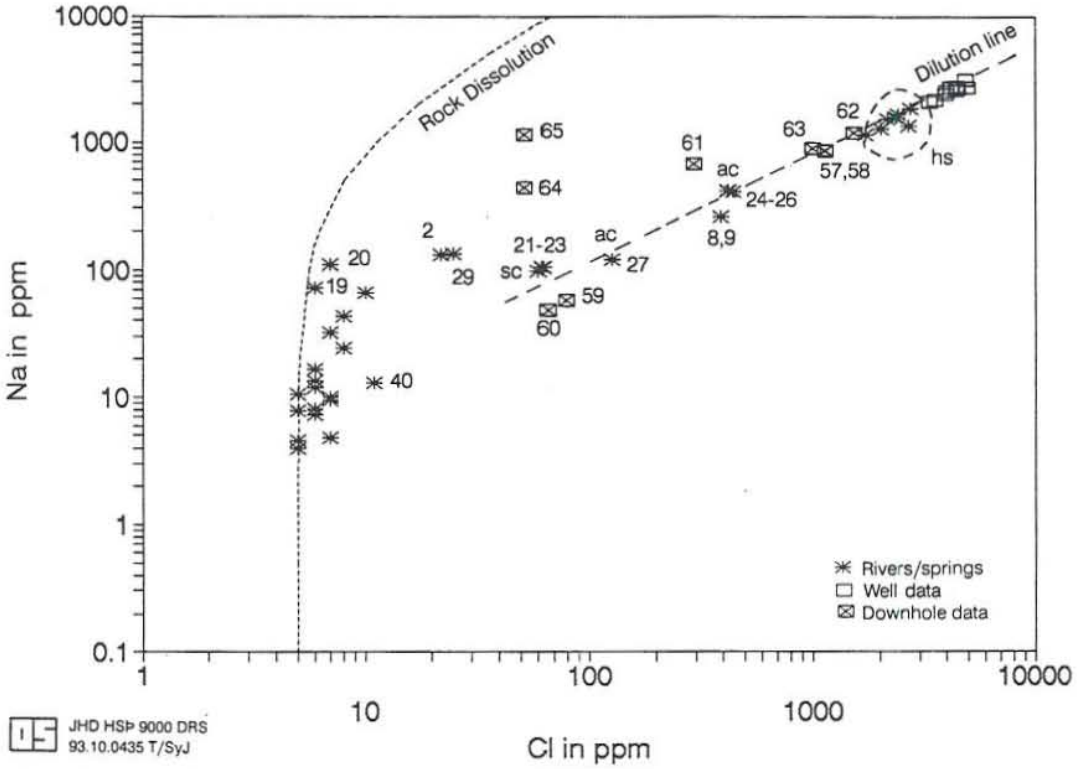

FIGURE 9: The distribution of rock-derived Na vs. total Cl in natural waters at Mt. Labo; as in Figure 8 the line represents the respective ratio (Na/Cl = 160) in andesitic rock

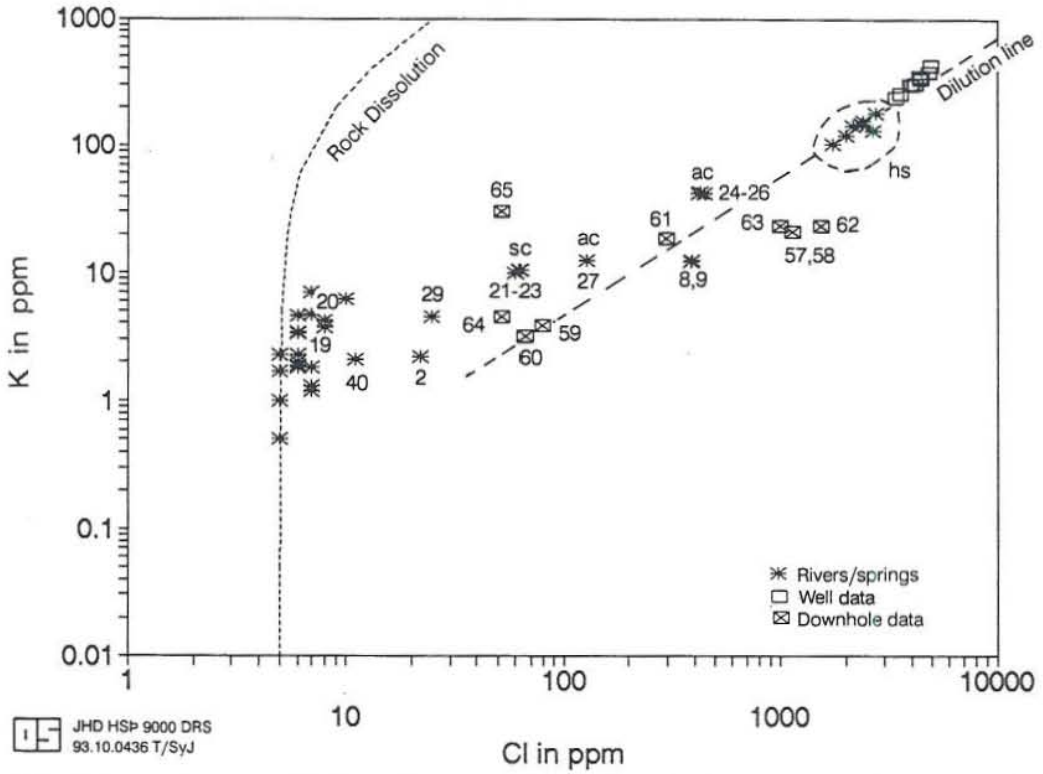

FIGURE 10: The distribution of rock-derived K vs. total Cl in natural water at Mt. Labo; as in Figure 8 the line represents the respective ratio (K/Cl = 50) in andesitic rock

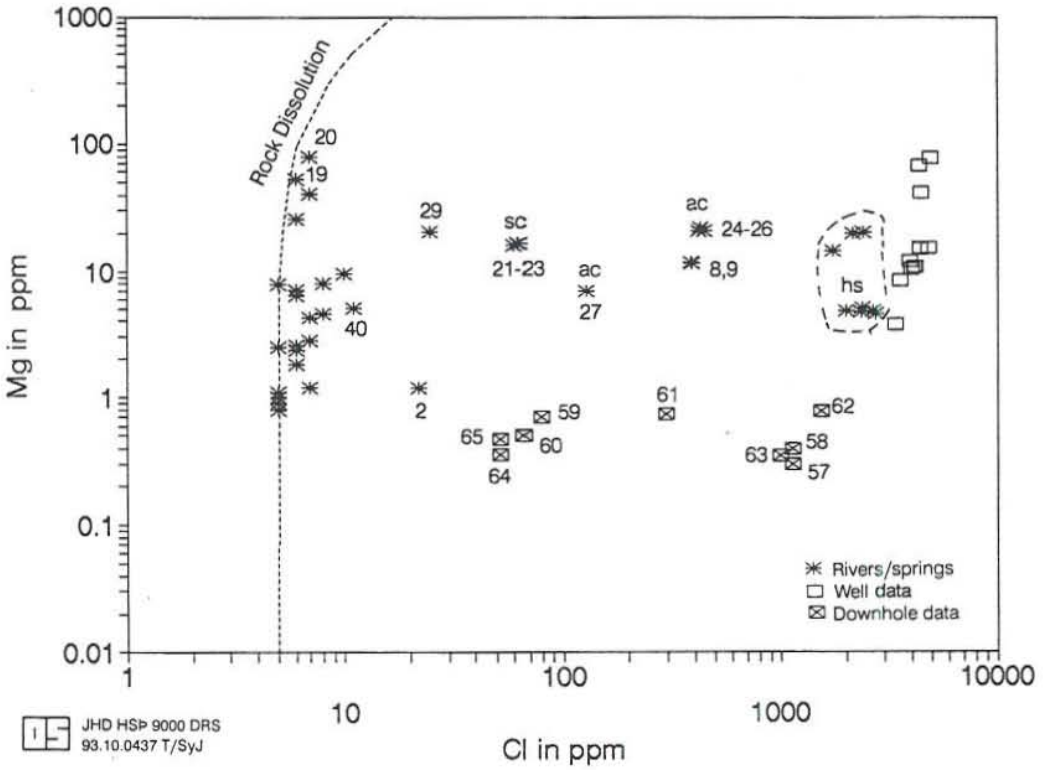

FIGURE 11: The distribution of rock-derived Mg vs. total Cl in natural waters at Mt. Labo; as in Figure 8 the line represents the respective ratio (Mg/Cl = 84) in andesitic rock

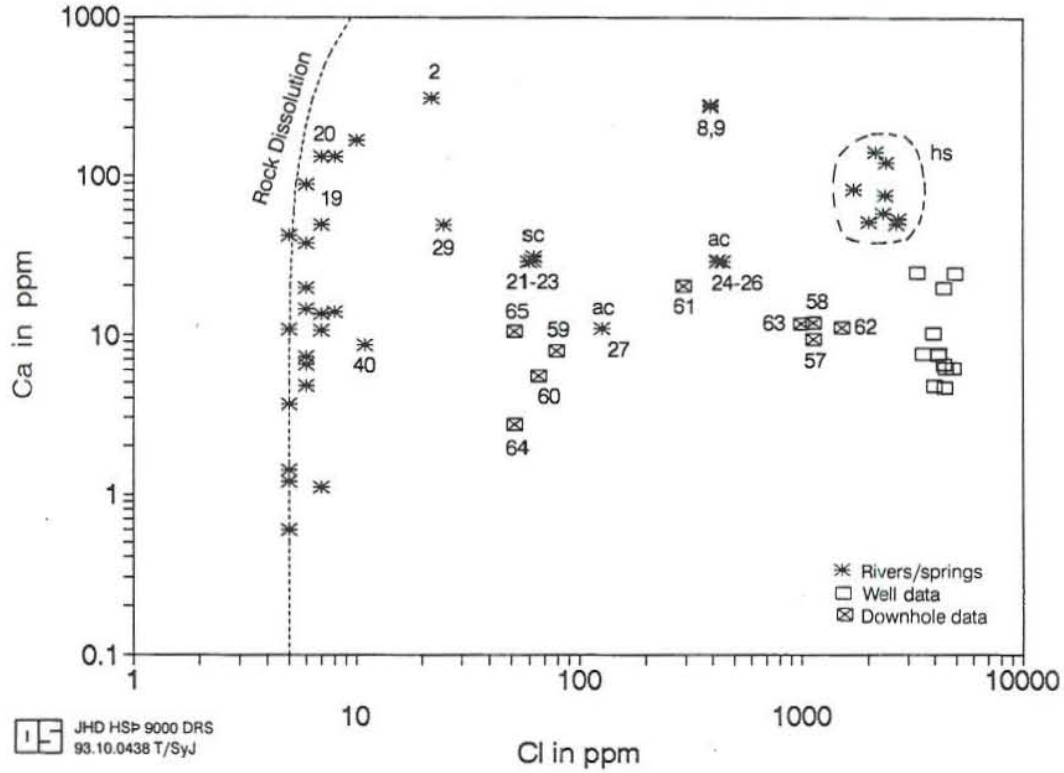

FIGURE 12: The distribution of rock-derived Ca and total Cl in natural waters at Mt. Labo; as in Figure 8 the line represents the respective ratio (Ca/Cl = 222) in andesitic rock

In Figure 11, Mg concentrations in the hot springs are similar to those of the well waters, indicating that Mg is not much affected by reactions in the upflow. On the other hand, it is seen from Figure 12 that Ca concentrations in the hot springs are considerably higher than in the wells, indicating dissolution in the upflow and reduced, if any, secondary mineral precipitation. Considering Ca to be in equilibrium with anhydrite ($CaSO_4$) and calcite ($CaCO_3$), its increased concentrations could also be the result of increasing solubility of both minerals with falling temperature in the upflow.

In Figure 13, the rock dissolution line is generated using the CO_2/Cl mass ratio of 4.0 from Hoefs (1974). It can be seen that the warm springs (2, 8-9, 21-23, and 29) and the well waters plot close to the CO_2/Cl rock dissolution line. This could be a mere coincidence or it could indicate that the CO_2/Cl ratio of the magma source is the same as that of the rock and that a small fraction of the CO_2 is removed from solution. The surface waters and cold springs (unlabelled asterisks) plot to the left of the line, indicating that they contain CO_2 in excess of that derived from the rock through stoichiometric dissolution. The additional source of CO_2 is considered to be the atmosphere, and, in particular, decaying organic matter in the soil. The hot spring waters, however, fall below the line, indicating loss of CO_2 from solution, probably through calcite precipitation.

5.2.2 Log Q diagrams and geothermometry

The WATCH programme (Arnorsson et al., 1982) has been used to evaluate the state of saturation of the rivers/springs and well fluids relative to selected hydrothermal minerals. The state of saturation can be evaluated by comparing Q (reaction quotient) and K (equilibrium constant) values. The general expression for the Gibbs free energy (ΔG) of a chemical reaction is given by:

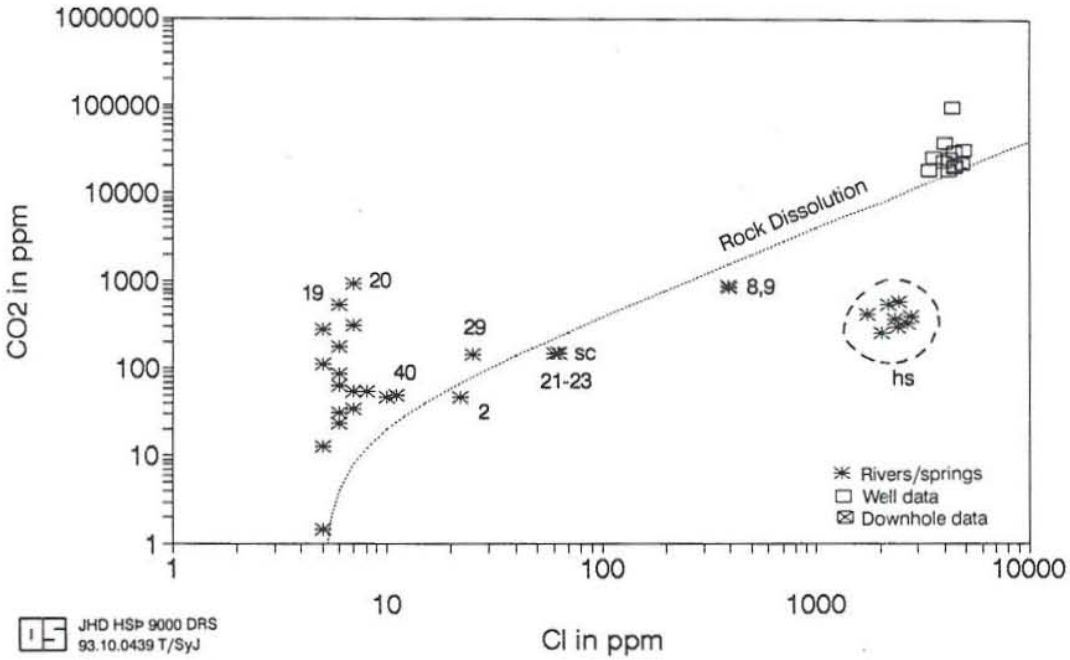

FIGURE 13: The distribution of rock- and soil-derived CO_2 vs. total Cl in natural water at Mt. Labo; as in Figure 8 the line represents the respective ratio (CO_2/Cl = 4) in andesitic rock

$$\Delta G = -RT\ lnK + RT\ lnQ \qquad (12)$$

R represents the gas constant and T is the temperature in Kelvin. K is the equilibrium constant and Q the reaction quotient. At equilibrium, $\Delta G = 0$, so $Q = K$. When reactions involving minerals and aqueous solutions are written in terms of dissolution, $Q>K$ in case of supersaturation, and $Q<K$ in case of undersaturation.

Plots of log Q versus temperature are shown in Figures 14 to 19. The log Q values corresponding to individual samples are represented by symbols, while the temperature dependence of the equilibrium constant is represented by lines.

SiO_2

There are two silica minerals that are known to control aqueous silica activities in geothermal waters, quartz and chalcedony. Their solubility is shown in Figure 14 together with the logarithm of the aqueous SiO_2 activities of the well and spring waters. The quartz and chalcedony solubility data are from Fournier and Potter (1982), and Fournier (1977), respectively. The selected temperatures are measured temperatures of spring discharges and measured aquifer temperatures for wells. Temperatures at points where downhole samples were collected are not available. For this reason these samples have not been plotted in Figure 14.

In Figure 14 the data points for the hot springs are above the saturation line, indicating that the waters in these hot springs are supersaturated relative to quartz. However, the well fluids plot close to the quartz solubility curve, indicating that the water at depth is close to equilibrium with quartz. The close alignment of some of the hot springs (5-7) with the chalcedony saturation line indicates that these waters have attained equilibrium with chalcedony at the prevailing discharge temperatures. If these waters have attained the temperature observed at depth in the wells, the hot spring waters must have lost a considerable amount of silica in the upflow through precipitation, yet not sufficient to attain equilibrium with quartz at the spring discharge temperatures, and generally not with chalcedony either.

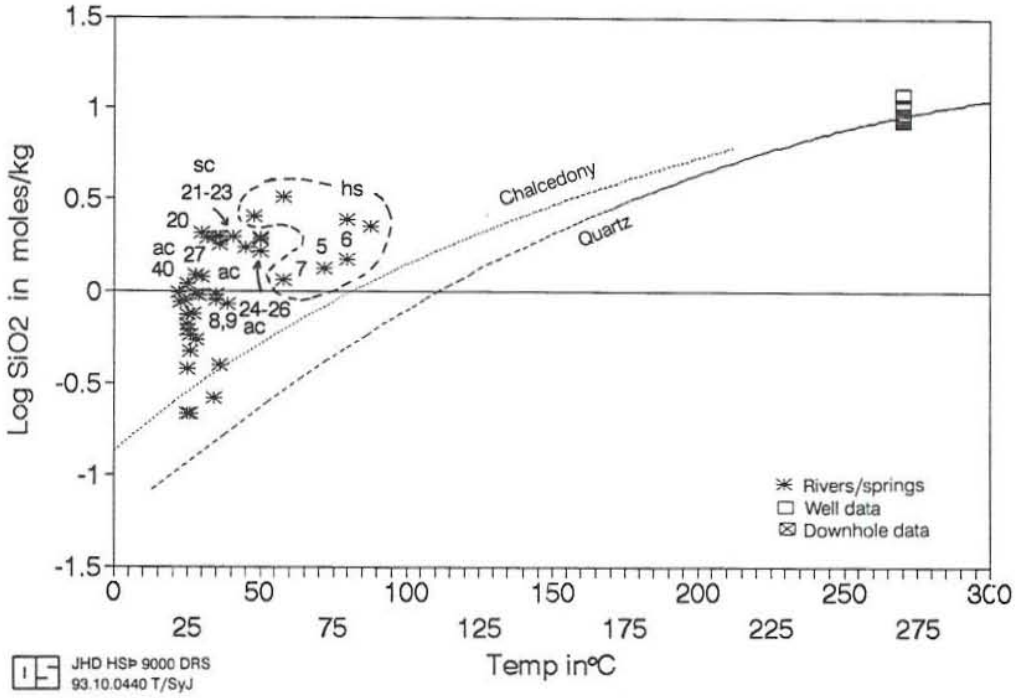

FIGURE 14: The chalcedony and quartz saturation state in natural waters at Mt. Labo; the respective solubility curves are from Fournier and Potter (1982), and Fournier (1977). The selected temperatures are measured discharge temperatures for the springs and measured aquifer temperatures for the wells; no measured temperatures are available for the downhole samples

On the basis of the quartz solubility data of Fournier and Potter (1982), the last equilibration temperatures of the hot springs (5-7) are found to range from 120 to 130°C, while for the wells the measured temperature (270°C) is almost equal to the quartz equilibrium temperatures, ranging from 266 to 270°C.

Since the neutral pH alkali-Cl hot springs at Kilbay-Alawihaw originate from the same source as the well waters, as already discussed, the difference in the geothermometry results indicates that quartz has precipitated in significant amounts from the water feeding the hot springs, although dilution may also contribute. It is not known whether the dilution occurs during lateral flow or vertical ascent, nor is it known if the quartz precipitation occurs in response to cooling during the lateral or vertical flow. If cooling occurs during lateral flow from the heat source, drilling at the hot spring site may not yield temperatures much above those indicated by the quartz geothermometer. If, on the other hand, cooling occurs as the hot water ascends under the hot springs, deep drilling is expected to yield temperatures higher than those indicated by the quartz geothermometry.

Na, K, and Mg

Three figures have been constructed to investigate the pattern of Na, K, and Mg activities in the Labo area waters. In Figure 15, the logarithm of the Na/K mass ratio has been plotted against Cl. The Na/K rock ratio is also delineated to compare the relative deviation of Na/K ratios in the waters to those of andesitic rock. In Figure 16, the same Na/K ratios are plotted against temperature, together with equilibrium curves according to various researchers (Arnorsson, 1983; Giggenbach, 1988; Fournier and Truesdell, 1973). Figure 17 is the Na-K-Mg diagram of

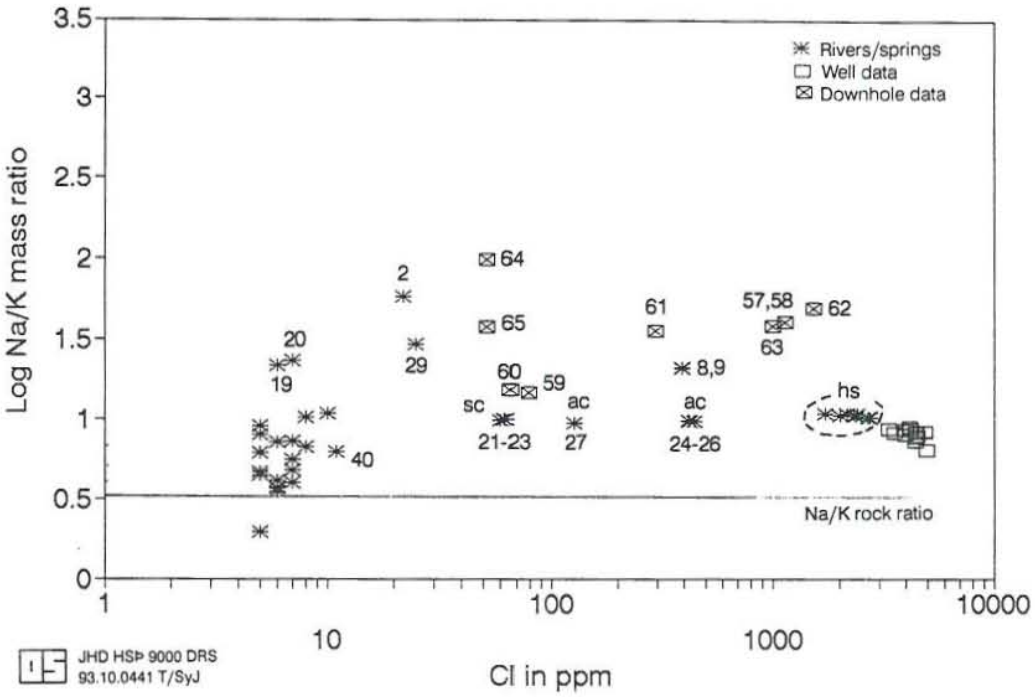

FIGURE 15: The distribution of log Na/K mass ratio vs. Cl; the rock dissolution line is delineated at log Na/K ratio of 0.50

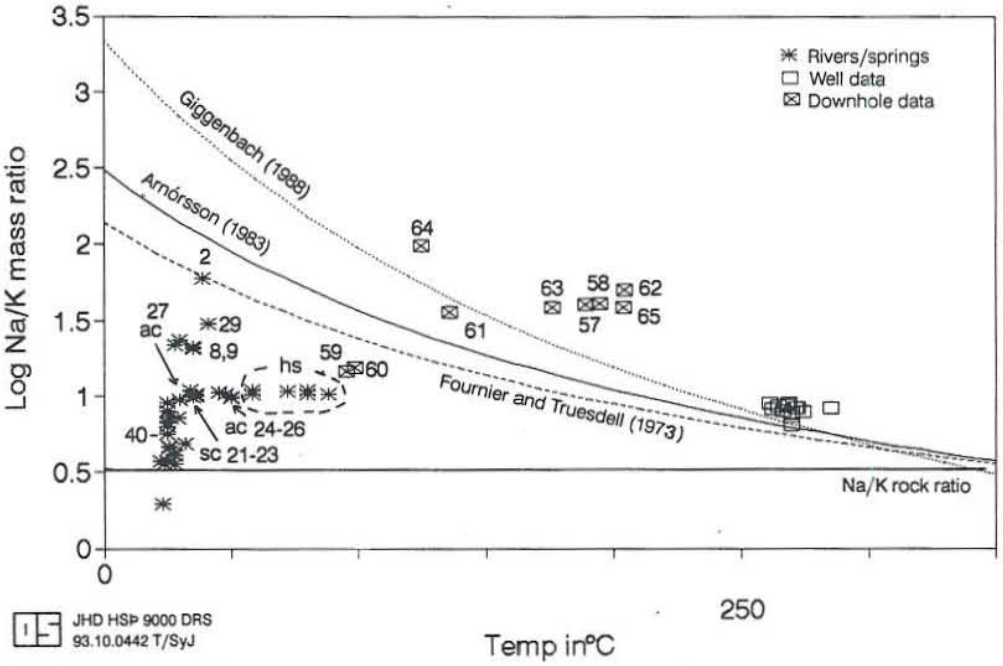

FIGURE 16: The distribution of log Na/K mass ratio vs. temperature; the rock dissolution line is delineated at log Na/K ratio of 0.50

Giggenbach (1988), showing relative equilibrium temperatures from the K-Na(t_{kn}) and K-Mg(t_{km}) geothermometers. The temperatures used for the rivers and springs are all measured temperatures, while for the well and downhole samples, quartz equilibrium temperatures were used.

In Figure 15, almost all the data points plot above the rock ratio, indicating that the Na and K

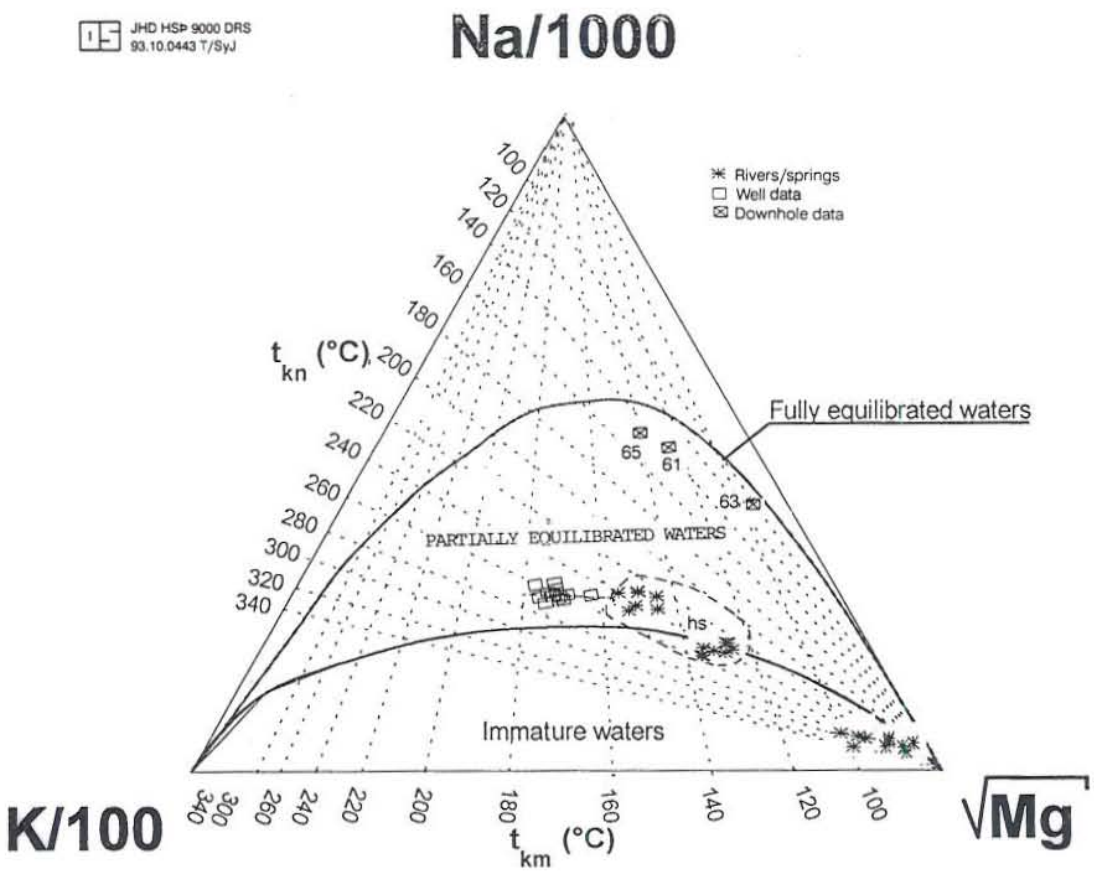

FIGURE 17: A plot of Mt. Labo waters on the Na-K-Mg ternary diagram of Giggenbach (1988), showing relative K-Na(t_{kn}) and K-Mg(t_{km}) temperatures

of the fluids are not controlled by stoichiometric rock dissolution, but probably by the precipitation of a secondary mineral. However, in Figure 16, almost all the rivers/springs and the hot spring data points plot much below the equilibrium lines, indicating that the Na and K of these waters have not equilibrated with low-albite and K-feldspar. The well fluids appear, on the other hand, to have attained equilibrium with both these minerals. Downhole samples show relatively high Na/K ratios for their quartz equilibrium temperatures. It is concluded that the Na and K in the rivers and springs are much affected by the dissolution process and are relatively far from equilibrium. As a result, their Na/K temperatures are high (>300°C), and meaningless.

Figure 17 shows a plot of the relative Mg, Na, and K concentrations in the Labo natural waters. The data points for the hot springs and the wells plot well below the "fully equilibrated line", indicating that the Mg is to some extent affected by the rock dissolution process and not by equilibrium with a secondary mineral. The partial equilibration of the well fluids is taken to indicate that Na and K have equilibrated, as shown in Figure 16, but that the Mg in the fluids has not, resulting in disequilibrium. This may be an artifact caused by the relatively low pH of the well waters, which enhances Mg mobility. The results for the hot springs, although not in equilibrium with low-albite and K-feldspar, indicate partial equilibration of the aqueous Mg with some mineral.

The estimated Na/K temperature (t_{kn}) of the well waters in Figure 17 is about 260°C, or not significantly lower than the measured temperatures of 270°C, indicating close approach to the equilibrium of the reservoir water with low-albite and K-feldspar.

Ca

The behaviour of Ca was investigated by plotting the calculated log Q values of anhydrite ($CaSO_4$) and calcite ($CaCO_3$), against temperature. The anhydrite and calcite equilibrium lines in Figures 18 and 19 were generated using the thermodynamic data of Helgeson (1969a, b) and Helgeson et al. (1978).

In Figure 18, much of the spring data are below the equilibrium line, indicating that the waters are anhydrite undersaturated. However, the well fluids and some of the downhole samples (57, 58, 62, and 65), are close to equilibrium with anhydrite, indicating that the activities of Ca and SO_4 are controlled by anhydrite solubility. It also indicates that some of the SO_4, resulting from dissolution of magmatic SO_2 in the geothermal water, has been precipitated to form anhydrite.

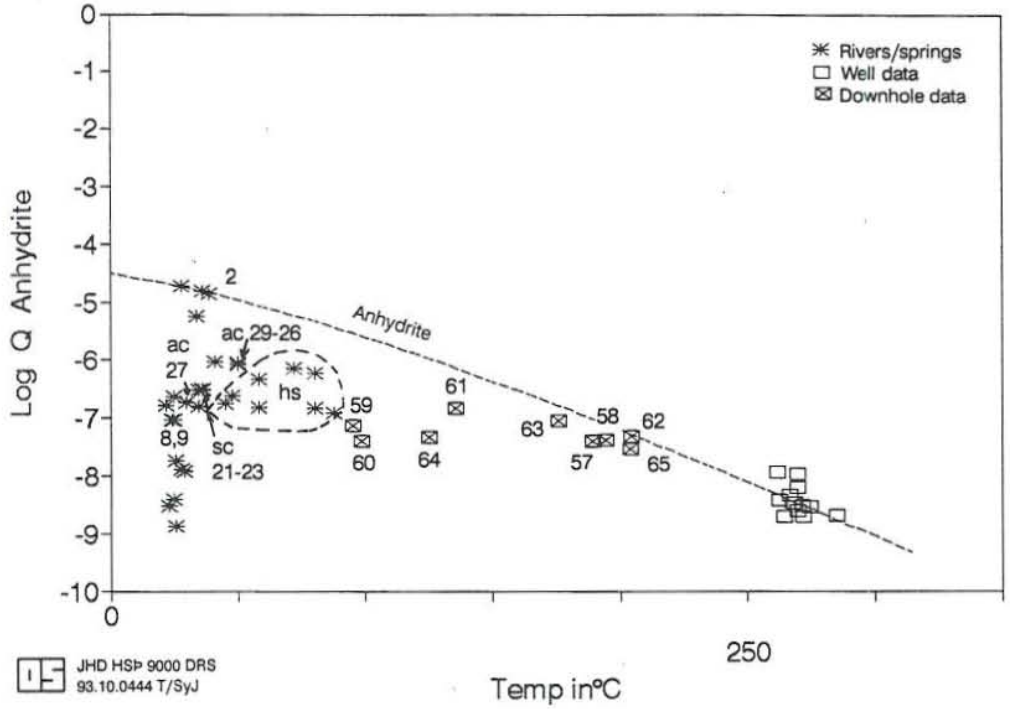

FIGURE 18: The anhydrite saturation state of natural waters at Mt. Labo; the anhydrite solubility curve is based on thermodynamic data from Helgeson (1969a, b) and Helgeson et al. (1978)

From Figure 19, it can be seen that the river waters and warm spring waters are undersaturated to somewhat supersaturated with respect to calcite, whereas all the hot springs are significantly supersaturated. The supersaturation is probably due to CO_2 degassing at shallow levels or in the conduit, either as a result of boiling or simply due to the formation of a separate gas phase as hydrostatic pressure is reduced on the rising hot water. The calculated calcite supersaturation of water in the hot springs is in line with observed calcite deposition around these springs. The well waters are somewhat calcite undersaturated. However, the calculated degree of undersaturation is probably not significant in view of all the uncertainties involved in calculating the calcium carbonate activity product.

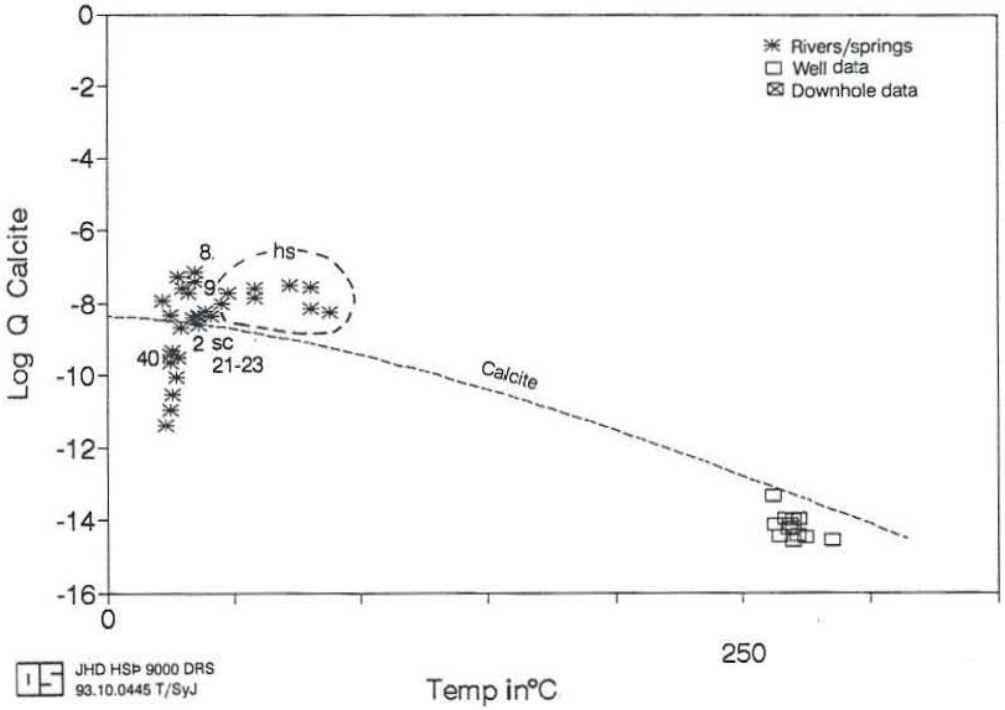

FIGURE 19: The calcite saturation state of natural waters at Mt. Labo; the calcite solubility curve is based on thermodynamic data from Helgeson (1969a, b) and Helgeson et al. (1978)

6. THE pH OF MT. LABO WATERS

Rock dissolution and hydrothermal alteration, i.e. precipitation of secondary minerals, involve uptake of protons and the simultaneous release of other cations as the primary constituents of the rock dissolve and secondary minerals precipitate (Gislason and Arnorsson, 1993). The alteration process may thus be described as hydrogen ion metasomatism. The water is "titrated" through dissolution of the igneous minerals and glass, which act as bases, thus causing the solution pH to rise (e.g. Sillen, 1961; Gislason and Eugster, 1987). Proton donors enhance the "titration" process. In surface waters, the source of protons is carbonic acid derived from atmospheric CO_2 and decay of organic matter.

In Mt. Labo, much of the surface waters and warm spring waters is high in total carbonate, ranging from 70 to 1300 ppm (calculated as HCO_3), with a neutral pH. This indicates that these waters are quite reactive, as is indeed substantiated by their relatively high concentration of cations, (Mg, Ca, K, and Na). However, the water from the Layaton Malaki cold spring (1) is very low in cations but it has a pH of 2.6. The reason for this has not been studied.

The concentrations of CO_2 and H_2S in thermal waters of high temperatures are much higher than those of warm waters, and they increase with increasing temperatures (Arnorsson and Gunnlaugsson, 1985). These gases form weak acids, which constitute the main proton donors in waters derived from high geothermal temperature (>150°C) heat sources. Their source could be the rock being dissolved or a degassing magma intrusion. The waters of the hot springs at Kilbay-Alawihaw could be considered as a product of such processes, with the magma probably being the main source of CO_2. The neutral pH of these waters could be attributed to extensive water-rock interaction leading to the destruction of these acids and the simultaneous formation of bicarbonate and sulphate ions, as reflected by the relatively high concentrations of SO_4, ranging from 100 to 400 ppm, and HCO_3, ranging from 400 to 800 ppm.

Magmatic gases from intrusive bodies are known to migrate into overlying groundwater systems, whether thermal or not (Arnorsson, 1986). These gases include CO_2, SO_2, and HCl, all of which are acid gases and therefore, upon dissolution, proton donors. The waters from the wells and from the acid to neutral pH SO_4-Cl springs (21, 24-27) could be considered products of this process. The dissolution of SO_2 and HCl, forming strong acids, would be the driving force in dissolving the primary minerals. During this process, the water is "titrated" through the dissolution of the igneous minerals and glass, which act as bases, thus causing the solution pH to rise. The calculated pH of 5.1 of the aquifer well fluids indicates that a large degree of rock "titration" has taken place, causing the pH to rise to almost neutral, leading to formation of some secondary minerals, such as quartz, low-albite, K-feldspar, calcite, and anhydrite, that control the activities of some major geoindicators in the system. The acid pH (pH<4.5) at the weirbox is not caused by an immediate intrusion of magmatic gases into the wellbore. It is caused by an increase in the dissociation constant of bisulphate ion, HSO_4^-, as the water cools by boiling, hence releasing a great amount of H^+, resulting in an acid pH. The HSO_4^- concentration in the well fluids ranges from 100 to 140 ppm (as computed from the WATCH programme), constituting almost 50% of the total SO_4 in the fluids. It is only natural that a high bisulphate-type water with close to neutral pH becomes acid on rising to cooler conditions at the surface.

7. SUMMARY AND CONCLUSIONS

The alkali-Cl hot springs at the Kilbay-Alawihaw have the same kind of source as the well fluids. It is not known if the hot springs are fed by a lateral flow from the drilled area in Mt. Labo, or from a separate source. Chemical geothermometry indicates aquifer temperatures of 120-130°C for the Kilbay-Alawihaw hot springs. Deep drilling at this site may not reveal higher temperatures, if the springs are connected to a lateral flow. If, on the other hand, the Kilbay-Alawihaw hot springs have a heat source separate from that of the wells, deep drilling may yield temperatures in excess of those predicted by chemical geothermometry.

Acid to neutral pH SO_4-Cl springs at Mabahong Labo have many chemical affinities similar to those of surface waters and cold groundwaters, affinities that indicate that they have not closely approached equilibrium with hydrothermal minerals. For this reason, geothermometry results at these springs are considered unreliable.

Surface waters possess Cl/B ratios in the range of 0.2 to 40, with Cl less than 10 ppm. Their B content ranges from 0.1 to 2.0 ppm. It is concluded that these waters have reacted substantially with the rock, and that most of the B must come from the rock, and some of the Cl. Neutral pH warm spring waters, that are dominated by the rock dissolution process, possess a Cl/B ratio of about 10, i.e. similar to andesitic rock. These waters have Cl concentrations ranging from 20 to 400 ppm, due to variable degree of rock dissolution.

Acid to neutral pH SO_4-Cl springs at Mabahong Labo are concluded to be the product of the mixing of magmatic gases with surface waters. It is estimated that the Cl derive from the magma heat source comprises 79-94% of the total Cl, while most of the B in the springs, 96-99%, comes from the rock.

The well fluids and the hot springs in Kilbay-Alawihaw are concluded to be the product of the mixing of magmatic gases with deep waters. It was calculated that about 94% of the total Cl in the well waters originates from the magma. For the hot springs, the figure is about 87%, indicating considerable rock-water interaction, subsequent to mixing. The source of B is, on the other hand, the dissolving rock, which contributes about 96% of the total B in the well fluids, and about 98% in the hot springs.

The dissolution of SO_2 and HCl from the degassing magma in the deep groundwater, forming strong acids, were concluded to be "titrated", through dissolution of the igneous minerals and glass. During this process, these minerals and glass act as bases, causing the pH to rise to almost neutral, and leading to the formation of secondary minerals, such as quartz, low-albite, K-feldspar, calcite, and anhydrite, that control the activities of some of the major geoindicators in the system. The apparent acid pH ($pH<4.5$) at the weirbox is not caused by an immediate intrusion of magmatic gases into the wellbore. It is caused by an increase in the dissociation constant of bisulphate ion, HSO_4^-, as the well fluids' temperature drops from 270 to 100°C during boiling in the well. This results in the release of a great guantity of H^+. The bisulphate in the well fluids ranges from 100 to 140 ppm, constituting 50% of the total SO_4. Thus, it is to be expected that a high bisulphate-type water of close to neutral pH becomes acid on rising to cooler conditions at the surface.

ACKNOWLEDGEMENTS

The author acknowledges the generosity of the Icelandic Government through the UNU Geothermal Training Programme here in Reykjavik, Iceland. The author is honoured for having been awarded the UNU Fellowship, and wishes to thank Dr. Ingvar B. Fridleifsson, Mr. Ludvik S. Georgsson, and Ms. Margret Westlund of the Training Programme for their guidance and support during his stay here. The adviser, Prof. Stefan Arnorsson, is greatly acknowledged for his patience and friendship throughout the preparation of this report. To the people of Orkustofnun, for such warm hospitality, which will always be treasured. Special thanks to the Nordic Institute of Volcanology, for the use of the library. And, to all UNU Fellows 1993, for such great company, thank you.

REFERENCES

Arnorsson, S., 1970: Underground temperatures in hydrothermal areas in Iceland as deduced from the silica content of the thermal water. Geothermics, Sp.is. 2, 1, 536-541.

Arnorsson, S., 1983: Chemical equilibria in Icelandic geothermal systems - Implications for chemical geothermometry investigations. Geothermics, 12, 119-128.

Arnorsson, S., 1985: The use of mixing models and chemical geothermometers for estimating underground temperatures in geothermal systems. J. Volc. Geothermal Res., 23, 299-335.

Arnorsson, S., 1986: Chemistry of gases associated with geothermal activity and volcanism in Iceland. A review. J. Geophys. Res., 91, 12261-12268.

Arnorsson, S., 1991: Geochemistry and geothermal resources in Iceland. In: D'Amore, F., (co-ordinator), Application of geochemistry in geothermal reservoir development. UNITAR/UNDP publication, Rome, 145-196.

Arnorsson, S., Andresdottir, A., and Sveinbjornsdottir, A.E., 1993: The distribution of Cl and B, δD, δ^{18}O in natural waters in the Southern Lowlands in Iceland. Geofluids '93, Extended Abstracts, 313-315.

Arnorsson, S., Gislason, S.R., Gestsdottir, K., and Oskarsson, N., 1989: Chlorine and boron in natural waters in Iceland. Proceedings of the 6th International Symposium on Water Rock Interaction, Malvern, England, 37-40.

Arnorsson, S., and Gunnlaugsson, E., 1985: New gas geothermometers for geothermal exploration - calibration and application. Geochim. Cosmochim. Acta, 49, 1307-1325.

Arnorsson, S., Gunnlaugsson, E., and Svavarsson, H., 1983: The chemistry of geothermal waters in Iceland. III. Chemical geothermometry in geothermal investigations. Geochim. Cosmochim. Acta, 47, 567-577.

Arnorsson, S., Sigurdsson, S., and Svavarsson, H., 1982: The chemistry of geothermal waters in Iceland. I. Calculation of aqueous speciation from 0 to 370°C. Geochim. Cosmochim. Acta, 46, 1513-1532.

BED (Bureau of Energy Development), 1986: Sedimentary basins of the Philippines - their geology and hydrocarbon potential, 2.

Biniza, E.M., 1990: LB-1D completion test. PNOC-EDC, internal report.

Clemente, V.C., 1990: A review of the geochemistry of the Mt. Labo geothermal prospect. PNOC-EDC, internal report.

D'Amore, F., 1991: Gas geochemistry as a link between geothermal exploration and exploitation. In: D'Amore, F. (co-ordinator), Application of Geochemistry in Reservoir Development. UNITAR/UNDP publication, Rome, 93-113.

Delfin, F.G., and Alincastre, R.S., 1988: Geology of Del Gallego (Mt. Labo) Geothermal Prospect, SE Luzon. PNOC-EDC, internal report.

Dizon, L.P., 1990: Paleoanalysis of well LB-2D. PNOC-EDC, internal report.

Ellis, A.J., 1970: Quantitative interpretation of chemical characteristics of hydrothermal systems. Geothermics, Sp.is. 2, 1, 516-528.

Ellis, A.J., and Mahon, W.A.J., 1964: Natural hydrothermal systems and experimental hot water-rock interactions. Geochim. Cosmochim. Acta, 28, 1323-1357.

Ellis, A.J., and Mahon, W.A.J., 1967: Natural hydrothermal systems and experimental hot water/rock interactions - part II. Geochim. Cosmochim. Acta, 31, 519-538.

Ellis, A.J., and Sewell, J.R., 1963: Boron in rocks and waters of New Zealand hydrothermal areas. N.Z.J. Sci., 6, 589-606.

Fournier, R.O., 1973: Silica in thermal waters: Laboratory and field investigations. Proceedings Internat. Symp. on Hydrogeochemistry and Biogeochemistry, Japan, The Clark Co., Washington D.C., 1, 122-139.

Fournier, R.O., 1977: Chemical geothermometers and mixing models for geothermal systems. Geothermics, 5, 41-50.

Fournier, R.O., 1979: Chemical and hydrological considerations of the use of enthalpy-chloride diagrams in the prediction of underground conditions in hot spring systems. J. Volc. Geothermal Res., 5, 1-16.

Fournier, R.O., 1991: Water geothermometers applied to geothermal energy. In: D'Amore, F. (co-ordinator), Application of geochemistry in geothermal reservoir development. UNITAR/UNDP publication, Rome, 37-66.

Fournier, R.O., and Potter, R.W., 1982: A revised and expanded silica (quartz) geothermometer. Geothermal Resources Council, Bulletin, 11-10, 3-12.

Fournier, R.O., and Truesdell, A.H., 1973: An Empirical Na-K-Ca geothermometer for natural waters. Geochim. Cosmochim. Acta, 37, 1255-1275.

Fuge, R., 1974: Chlorine. In: Wedephol, K.H. (editor), Handbook of geochemistry. Springer-Verlag, Berlin, 17-E-4.

Gerardo, J.Y., 1993: LB-1D Geochemistry. PNOC-EDC, internal report.

Giggenbach, W.F., 1988: Geothermal solute equilibria. Derivation of Na-K-Ca-Mg geoindicators. Geochim. Cosmochim. Acta, 52, 2749-2765.

Giggenbach, W.F., 1991: Chemical Techniques in geothermal exploration. In: D'Amore, F. (co-ordinator), Application of geochemistry in geothermal reservoir development. UNITAR/UNDP publication, Rome, 119-142.

Giggenbach, W.F., and Matsuo, S., 1991: Evaluation of results from the 2nd and 3rd IAVCEI Field Workshops on Volcanic Gases, Mt. Usu, Japan, and White Island, New Zealand. Appl. Geochem., 6, 125-141

Gislason, S.R., and Arnorsson, S., 1993: Dissolution of primary basaltic minerals in natural waters: Saturation state and kinetics. Chem. Geol., 105, 117-135.

Gislason, S.R., and Eugster, H.P., 1987: Meteoric water-basalt interactions. I. A laboratory study. Geochim. Cosmochim. Acta, 51, 2827-2840.

Harder, H., 1963: To what extent is boron a marine index element. Fortschr. Geol. Rheinld. u. Westf., 10, 239-253.

Harder, H., 1969: Boron. In: Wedephol, K.H. (editor), Handbook of geochemistry. Springer-Verlag, Berlin, II-1, 5-E-1 to 5-E-4.

Helgeson, H.C., 1969a: Thermodynamics of complex dissociation in aqueous solution at elevated temperatures and pressures. Amer. J. Sci., 267, 729-804.

Helgeson, H.C., 1969b: Thermodynamics of hydrothermal systems at elevated temperatures. J. Phys. Chem., 71, 729-804.

Helgeson, H.C., Delany, J.M., Nesbitt, H.W., and Bird, D.K., 1978: Summary and critique of the thermodynamic properties of rock-forming minerals. Amer. J. Sci., 278-A, 1-229.

Hoefs, J., 1974: Carbon. In: Wedephol, K.H. (editor), Handbook of geochemistry. Springer-Verlag, Berlin, II-2, 6-E-3.

Layugan, D.B., Maneja, F.C., and Fragata, J.J., 1988: Resistivity measurements at Del Gallego (Mt. Labo) geothermal Prospect, SE Luzon. PNOC-EDC, internal report.

Le Guern, F., and Bernard, A., 1982: A new method for sampling and analyzing sublimates. Application to Merapi volcano, Java. J. Volc. Geotherm. Res., 12, 133-146.

McBirney, A.R., 1984: Igneous petrology. Freeman, Cooper, & Co., San Francisco, CA, 313 pp.

Nemeto, T., Hayakawa, M., Takahashi, K., and Oana, S., 1957: Report on the geological, geophysical, and geochemical studies of Usu volcano (Showashinzan). Geol. Surv. Japan, report 170, 149 pp.

Palmer, M.R., Spivack, A.J., and Edmond, J.M., 1987: Temperature and pH controls over isotopic fractionation during absorption of boron on marine clays. Geochim. Cosmochim. Acta, 51, 2319-2323.

Panem, C.C., Maturgo, O.O., and Villarosa, H.A., 1990: Geology and petrology of well LB-1D. PNOC-EDC, internal report.

PNOC-EDC, 1991: Post-drilling geoscientific evaluation of the Mt. Labo geothermal project, Camarines Norte. PNOC-EDC, internal report.

Ramos, S.G., Malixi, L.V., and Espiridion, J.A., 1992: Geology and petrology of LB-3D. PNOC-EDC, internal report.

Reed, M.H., 1991: Computer modelling of chemical processes in geothermal systems: Examples of boiling, mixing, and water-rock reaction. In: D'Amore, F. (co-ordinator), Application of

geochemistry in geothermal reservoir development. UNITAR/UNDP publication, Rome, 275-295.

Sanchez, D.R., 1993: Geochemistry of LB-3D. PNOC-EDC, internal report.

Seyfried, W.E., Janecky, D.R., and Mottl, M.J., 1984: Alteration of the oceanic crust: Implications for geochemical cycles of lithium and boron. Geochim. Cosmochim. Acta, 46, 557-569.

Sillen, L.G., 1961: The physical chemistry of seawater. In: Sears, M. (editor), Oceanography. Am. Assoc. Adv. Sci., Washington, D.C., publ. 67, 549-581.

Spivack, A.J., Palmer, M.R., and Edmond, J.M., 1987: The sedimentary cycles of boron isotopes. Cosmochim. Geochim. Acta, 51, 1939-1950.

Stefansson, V., and Arnorsson, S., 1975: A comparative study of hot-water chemistry and bedrock resistivity in the Southern Lowlands of Iceland. Proceedings of the 2nd United Nations Symposium on the Development and Use of Geothermal Resources, 1207-1216.

Symonds, R.B., 1992: Getting the gold from the gas: How recent advances in volcanic-gas research have provided new insight on metal transport in magmatic fluids. Geol. Surv. Japan, report 279, 170-175.

Symonds, R.B., Reed, M.H., and Rose, W.I., 1992: Origin, speciation, and fluxes of trace element gases at Augustine volcano, Alaska: Insights into magma degassing and fumarolic processes. Geochim. Cosmochim. Acta, 56, 633-657.

Symonds, R.B., Rose, W.I., Reed, M.H., Lichte, F.E., and Finnegan, D.L., 1987: Volatilization, transport and sublimation of metallic and non-metallic elements in high temperature gases at Merapi Volcano, Indonesia. Geochim. Cosmochim. Acta, 51, 2983-2101.

Tebar H.J., and Apuada N.A., 1985: Mt. Labo surface geology. PNOC-EDC, internal report.

Truesdell, A.H., 1975: Summary of section III - Geochemical techniques in exploration. Proceedings of the 2nd United Nations Symposium on the Development and Use of Geothermal Resources, San Francisco, 1, liii-lxxix.

Truesdell, A.H., 1991: Effects of physical processes on geothermal fluids. In: D'Amore, F. (co-ordinator), Application of geochemistry in geothermal reservoir development. UNITAR/UNDP publication, Rome, 71-92.

White, D.E., 1970: Geochemistry applied to discovery, evaluation, and exploitation of geothermal energy resources. Geothermics, Sp.Is. 2, 1, 58-80.

APPENDIX I: The chemical composition (in ppm) of natural waters at Mt. Labo

A. Chemistry of rivers and springs

Source	MMDDYY	No. code	Temp in C	pH / Temp C	B	SiO2	Na	K	Mg	Ca	Cl	SO4	Fe	HCO3	CO2T
LAYATON MALAKI		1	28	2.620 / 28	0.350	33.0	4.8	1.2	1.2	1.1	7	105	15.80	ND	ND
MOCBOC		2	39	7.588 / 39	2.340	51.0	130.0	2.2	1.2	313.0	22	960	0.10	65	48.885
NATULDUCAN		3	34	7.601 / 34	2.420	15.8	66.0	6.1	9.6	166.0	10	527	2.18	65	48.885
NABANGIKA	092487	4	36	7.663 / 36	0.860	24.0	43.5	4.2	8.1	133.0	8	375	1.25	76	54.819
KILBAY HS 1	051987	5	72	7.686 / 72	30.700	80.3	1539.0	143	20	140.0	2172	226	2.36	732	527.99
KILBAY HS 2	051987	6	80	7.662 / 80	33.500	90.2	1675.0	155	20.2	122.0	2417	240	2.45	819	590.74
KILBAY HS 3	051987	7	58	7.851 / 58	24.300	69.8	1125.0	103	14.4	82.5	1731	175	0.88	576	415.47
BAAY 1	032387	8	35	7.231 / 35	44.900	54.1	261.0	12.5	11.6	280.0	391	12	1.25	1143	824.45
BAAY 2	032387	9	35	7.472 / 35	43.200	58.4	261.0	12.3	11.7	272.0	389	12	1.39	1199	864.84
KAGUPGUPAN	052387	10	28	7.275 / 28	1.040	58.3	12.0	3.4	7.1	14.3	6	6	0.22	86	62.032
ALAWIHAW 1	052287	11	58	7.823 / 58	35.700	196.0	1852.0	180	4.6	53.2	2758	105	0.46	543	391.67
ALAWIHAW 2	052287	12	48	7.912 / 48	29.400	153.0	1560.0	150	5.1	76.2	2389	97	0.74	419	302.22
ALAWIHAW 3	052287	13	88	7.518 / 88	28.900	136.0	1340.0	131	4.9	50.1	2670	97	1.29	460	331.8
ALAWIHAW 4	052287	14	45	7.829 / 45	24.100	105.0	1268.0	121	4.9	50.4	2010	91	0.27	356	256.78
ALAWIHAW 5	052287	15	80	7.542 / 80	29.800	148.0	1550.0	149	4.8	58.4	2345	98	0.60	508	366.42
KATIGBIGAN		16	26	7.000 / 26	0.610	28.4	7.9	1.7	2.5	10.8	5	12	0.38	395	284.91
KAMPOSTA		17	26	2.670 / 26	0.610	13.0	4.5	1	1.1	0.6	5	15	0.06	ND	ND
MANIKPIK SEEPAGE		18	25	3.010 / 25	0.430	13.0	4.0	0.5	0.9	1.4	5	16	0.82	ND	ND
ALINSANAY 2	032887	19	28	7.984 / 28	21.400	73.9	72.5	3.3	53	87.6	6	ND	2.63	714	515.01
ALINSANAY 1	032887	20	30	7.305 / 30	36.500	124.0	110.0	4.7	79.4	131.0	7	ND	3.87	1304	940.56
L.MABAHONG LABO	032787	21	35	7.704 / 35	0.520	119.0	98.0	10	16.2	28.7	60	107	0.00	207	149.31
L.MABAHONG LABO	032787	22	36	7.567 / 36	7.350	119.0	103.0	10.4	16.8	29.2	62	109	0.08	210	151.47
L.MABAHONG LABO	032787	23	36	7.609 / 36	7.780	108.0	103.0	10.4	16.9	30.5	63	111	0.00	206	148.59
U.MABAHONG LABO	032787	24	50	3.527 / 50	2.680	115.0	408.0	42.3	21.3	28.4	446	609	0.21	ND	ND
U.MABAHONG LABO	032787	25	50	3.544 / 50	2.590	118.0	417.0	43.5	21.9	29.2	427	574	0.20	ND	ND
U.MABAHONG LABO	032787	26	50	3.384 / 50	2.680	99.1	416.0	42.7	21.2	28.5	420	587	0.26	ND	ND
U.MABAHONG LABO	032787	27	30	3.146 / 30	2.730	73.1	119.0	12.6	6.9	11.0	128	172	0.13	ND	ND
BAYBAY	093087	28	29	7.792 / 29	0.260	57.1	13.5	1.9	6.4	19.9	6	4	ND	119	85.835
PAGTIGBUNGAN	032987	29	41	7.611 / 41	9.950	119.0	134.0	4.5	20.9	48.9	25	246	ND	201	144.98
WALA 1	092987	30	25	3.180 / 25	0.350	40.0	24.5	3.7	4.6	13.8	8	135	4.00	ND	ND
WALA 2		31	23	6.770 / 23	0.610	52.4	4.5	2.3	0.8	3.7	5	4	0.00	18	12.983
WALA 3		32	24	2.510 / 24	0.350	54.3	8.1	2.3	1.8	4.8	6	205	43.60	ND	ND
HAGDAN 1	100487	33	32	7.930 / 32	0.170	117.0	32.8	6.9	40.3	49.1	7	18	1.81	424	305.83
HAGDAN 2		34	22	8.068 / 22	0.170	59.0	16.8	4.8	26.2	37.6	6	41	0.00	248	178.88
BACOCO RIVER	052087	35	25	7.760 / 25	1.730	22.8	10.5	1.7	7.9	41.9	5	17	0.10	157	113.24
MANIKPIK RIVER		36	25	4.160 / 25	0.430	13.0	4.5	0.5	1	1.2	5	6	0.09	2	1.4426
LAYATON MAUIT		37	25	7.470 / 25	1.380	45.0	10.0	1.8	4.3	13.5	7	5	0.00	74	53.376
LAYATON RIVER		38	26	6.740 / 26	0.660	35.0	9.5	1.3	2.8	10.6	7	9	0.11	48	34.622
KAMPOSTA RIVER		39	25	6.640 / 25	0.660	37.0	7.4	2	2.6	7.3	6	7	0.11	33	23.803
BALUJAG		40	25	7.490 / 25	1.360	67.0	13.0	2.1	5.1	8.7	11	51	0.09	66	49.046
GALLEGO	100787	41	no data	8.030 / no data	0.520	34.3	244.0	20.2	16.7	53.9	237	150	0.27	347	250.29
GALLEGO		42	no data	no data / no data	ND	31.4	36.5	4.9	4.6	8.0	ND	47	0.53	ND	ND
MALABTUG RIVER	032487	43	27	7.380 / 27	1.780	45.5	7.4	1.8	2.4	6.5	6	ND	0.18	43	31.016

B. Chemistry of Mt. Labo Geothermal wells

Source	MMDDYY	No. code	Temp in C	pH	/ Temp C	B	SiO2	Na	K	Mg	Ca	Cl	SO4	Fe	F	CO2T	H2S	NH3	O2	CH4	N2
LB3DX18	111092	44	262	5.219	/ 262	21.78	517	2070	236	3.61	24.40	3368	318	1.100	ND	18479	475	ND	2.85	65.60	42.48
19	111092	45	262	5.007	/ 262	23.04	520	2117	260	8.40	7.60	3543	380	0.657	ND	25760	664	ND	3.98	91.74	59.41
31	111692	46	264	4.921	/ 264	23.66	531	2543	298	10.40	4.80	3989	426	0.500	0.850	37191	1103	3.14	5.00	80.23	73.57
32	111692	47	267	5.113	/ 267	24.54	539	2390	301	12.10	10.23	3973	426	0.680	0.880	22809	675	0.00	3.06	49.12	45.25
45	112492	48	268	5.045	/ 268	27.07	545	2671	306	10.90	7.58	4185	462	0.705	0.825	24913	740	2.91	11.10	47.80	67.30
46	112492	49	269	5.174	/ 269	27.62	547	2705	305	10.90	7.50	4163	457	1.313	0.853	18280	543	3.12	8.29	35.80	50.29
82	121092	50	271	5.086	/ 271	19.55	559	2744	331	15.10	6.50	4405	507	1.450	0.823	19910	556	3.67	15.02	24.39	46.75
84	121192	51	285	5.202	/ 285	21.66	616	3084	374	15.30	6.22	4823	579	1.310	0.926	22340	766	4.47	21.51	35.56	57.69
88	121292	52	272	5.449	/ 272	26.91	563	2731	335	15.40	4.69	4432	570	10.300	0.938	20642	635	4.08	19.19	31.05	56.08
96	121692	53	275	5.096	/ 275	22.62	573	2659	338	41.70	6.20	4485	604	3.140	0.818	21178	647	ND	10.38	29.70	47.73
99	121892	54	270	4.975	/ 270	22.14	553	2627	344	15.00	4.69	4436	644	4.460	0.846	30448	930	2.55	14.93	42.70	68.63
LB1D-X-7	102292	55	270	4.892	/ 270	41.69	727	2677	423	78.30	24.33	4943	716	95.350	NA	31010	979	2.46	NA	NA	NA
LB1D-X-2	102292	56	270	4.611	/ 270	36.69	639	2554	350	67.70	19.70	4386	629	20.120	NA	95102	1094	3.74	NA	NA	NA
LB1D 1DH AT 1800	120190	57	189	6.127	/ 189	22.50	227	853	21	0.30	9.50	1142	236	NA	NA	NA	NA	NA	NA	NA	NA
	120190	58	194	7.045	/ 194	18.20	250	857	21	0.40	12.00	1142	195	NA	NA	NA	NA	NA	NA	NA	NA
LB1D 1DH AT 2500	120190	59	95	4.843	/ 95	2.30	43	57	4	0.70	8.00	79	78	NA	NA	NA	NA	NA	NA	NA	NA
	120190	60	98	5.363	/ 98	1.70	46	49	3	0.50	5.50	66	56	NA	NA	NA	NA	NA	NA	NA	NA
LB1D 2DH AT 1800	082992	61	136	6.210	/ 136	1.90	98	672	19	0.75	20.20	299	1134	23.100	NA	NA	NA	NA	NA	NA	NA
	090292	62	205	6.180	/ 205	7.30	279	1175	24	0.78	11.20	1547	460	16.200	NA	NA	NA	NA	NA	NA	NA
	090292	63	176	6.112	/ 176	7.40	188	904	24	0.35	11.80	1000	466	13.200	NA	NA	NA	NA	NA	NA	NA
LB1D 2DH AT 2500	090192	64	125	7.946	/ 125	0.30	94	441	4	0.36	2.70	52	388	3.200	NA	NA	NA	NA	NA	NA	NA
	090292	65	204	6.060	/ 204	4.50	277	1147	30	0.47	10.50	52	220	11.800	NA	NA	NA	NA	NA	NA	NA

Note:

1. Temperatures of the rivers and springs are measured temperatures.
2. Temperatures of the wells and downhole samples are in Tqtz of Fournier and Potter (1982).
3. Aquifer measured temperature of the wells is 270 C.
4. Sampling depths of the downhole samples (DH) are in mVD (meters-vertical-depth) from the surface.
5. NA means not analyzed; ND means not detected.